

國立交通大學  
顯示科技研究所

碩士論文  
紫外光於 PMMA 有機薄膜電晶體  
之光響應提升研究



UV-enhanced Photo responsivity on  
PMMA-OTFTs

研究生：顏睿志

指導教授：冉曉雯 博士

中華民國 九十六年 六月

紫外光於 PMMA 有機薄膜電晶體之光響應提升研究

UV-enhanced Photo responsivity on PMMA-OTFTs

研究生：顏睿志

Student : Ruei-Chih Yan

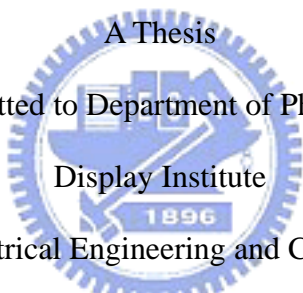
指導教授：冉曉雯 博士

Advisor : Dr. Hsiao-Wen Zan

國立交通大學

光電工程學系 顯示科技研究所

碩士論文



A Thesis  
Submitted to Department of Photonics  
Display Institute  
1896  
College of Electrical Engineering and Computer Science  
National Chiao Tung University  
in partial Fulfillment of the Requirements  
for the Degree of  
Master  
in  
Electro-Optical Engineering  
June 2007  
Hsinchu, Taiwan, Republic of China

中華民國九十六年六月

# 紫外光於 PMMA 有機薄膜電晶體之光響應提升研究

研究生:顏睿志

指導教授:冉曉雯 博士

國立交通大學

顯示科技研究所碩士班

## 摘要

在本研究中，以加熱固化的方式，將可溶性的甲基丙烯酸甲酯製作成有機薄膜電晶體的閘極介電層。並利用紫外光，對甲基丙烯酸甲酯一閘極介電層進行改質。根據觀察，經過紫外光改質後的閘極介電層，有機薄膜電晶體的臨界電壓將會降低、次臨界幅擺增加、而載子的場效飄移率則沒有顯著的變化。在光照射有機薄膜電晶體的實驗中，以波長為 460 奈米的光線對元件進行照射。經過紫外光改質後的元件，光照射時會觀察到一個較大的臨界電壓飄移與光響應。若對光照特性進行時間相依的分析，則發現紫外光改質後的元件有較短的飽和時間與較長的回復時間。為找出紫外光改質影響元件特性差異的原由，我們藉著材料分析與介電層的漏電分析，各自排除紫外光改質後影響有機半導體膜內部結構與介電層內產生捕捉缺陷，而主導特性差異的可能性。最後，我們推測元件電特性的差異可能是來自於半導體與介電層間、因紫外光改質而產生界面的捕捉缺陷態所主導。並以一系列的時間常數特性來加以驗證提出的假設。

# UV-enhanced Photo responsivity on PMMA-OTFTs

Student:Ruei-Chih Yan

Advisor:Dr. Hsiao-Wen Zan

Display Institute

National Chiao Tung University

## Abstract

In this study, with the thermal solidification method, the soluble Polymethylmethacrylate (PMMA) was used as the gate-dielectric of organic thin film transistors (OTFTs). Furthermore, we treated the PMMA gate-dielectric with the UV-light treatment. According to our observation, the OTFTs with UV-light treatment on gate-dielectric, the threshold voltage will be reduced, the subthreshold swing will be increased, however, no significant change in field-effect mobility was observed. In the OTFT experiments under light-irradiation, the devices was irradiated with a ray at a wavelength about 460nm. Among the OTFTs with UV-light treatment on gate-dielectric, when the light-irradiation was turn on, a larger threshold voltage shift and phonic responsivity will be found. If we further analyzed the time-dependent OTFT characteristics after the light-irradiation, the OTFTs with UV-light treatment will show a shorter saturation time and a longer recovering time.

In order to find out the origin of UV-light treatment on OTFT property variation, we tried to introduce the material analysis and dielectric-leakage analysis to rule out the effects of UV-light treatment on organic semiconductor inertial structure and the traps inside the dielectric film, respectively. Finally, we presumed the OTFT property variation should be dominated by the interface traps between the organic semiconductor film and the dielectric film, which may be created by the UV-light treatment. The proposed assumption is also verified by a serious time-constant analysis.



# 誌謝

兩年時間的飛逝，回首兩年前，懷抱著期望與夢想進入交大。在求學過程中，遇到了許多困難與考驗，這些考驗使自己在思想或能力上都成長許多。首先要感謝我的指導教授冉曉雯老師，感謝冉老師帶領我進入 OTFT 的領域，使我有機會在這塊領域著墨，並從研究當中讓我了解到一個研究者該有的執著與專業。

感謝實驗室的博班學長：國錫學長、政偉學長、士欽學長，在這兩年來的幫助與鼓勵。尤其是國錫學長，在我這兩年來的研究生涯裡，用心的教導我實驗方法提供實驗上的想法，並在心情低落時給予我適時的開導，且不辭辛勞地協助我完成我的碩士論文。也要感謝實驗室的同學：光明、而康、德倫以及同為 OTFT 組的皇維、廷遠、芸嘉、文馨，這兩年來的互相打氣，互相砥礪，一起努力堅持到最後。有你們的陪伴，讓我在這兩年研究生涯中更為甘甜回味。

最後感謝我的父母，感謝你們一路的陪伴與支持，沒有你們，就不會有今日的我。

# Contents

<b>Abstract (Chinese)</b>	I
<b>Abstract (English)</b>	II
<b>Acknowledgement</b>	IV
<b>Contents</b>	V
<b>Table Captions</b>	VII
<b>Figure Captions</b>	VIII
<b>Chapter 1. Introduction</b>	
1-1 Introduction of Organic Thin Film Transistors (OTFTs)	1
1-2 Spin-on Coated Dielectrics	2
1-3 Application of Organic Transistors to Optical Devices	3
1-4 Motivation	3
1-5 Thesis Organization	4
<b>Chapter 2. Theoretical Background of OTFTs</b>	
2-1 Introduction	5
2-2 Transportation Mechanisms of Organic Semiconductor	5
2-3 Photonic excitation on Organic Devices	8
2-4 Parameter Extraction	11
2-4-1 Mobility	11
2-4-2 Threshold voltage	12
2-4-3 Subthreshold swing	12
2-4-4 Responsivity	13
<b>Chapter 3. Experiments</b>	
3-1 PMMA Dielectric Fabrication and UV-light Treatment	14
3-2 PMMA-OTFTs Fabrication	14
3-3 Photonic excitation	16
<b>Chapter 4. Result and Discussion</b>	
4-1 Electrical Properties of PMMA Dielectric	17
4-1-1 Fabrication of PMMA dielectrics and relative dielectric properties	17
4-1-2 UV treatment on PMMA dielectric	18

4-2 Characteristics of OTFTs with distinct PMMA-dielectrics	19
4-3 Characteristics of light-illumination on PMMA-OTFTs	20
4-4 Time-dependent parameter analysis under and after light-illumination	21
4-5 Material analysis on PMMA-OTFTs	23
4-6 Plausible origin of the enhancement on photo responsivity	25

## **Chapter 5. Conclusion**

5-1 Conclusion	28
----------------	----

<b>References</b>	30
-------------------	----

<b>Tables</b>	34
---------------	----

<b>Figures</b>	37
----------------	----

<b>Profile</b>	56
----------------	----





# Table Captions

Table I The comparison of the different polymer OTFTs electrical properties.

Table II The comparison of untreated and UV-treated PMMA dielectrics properties.

Table III Time dependent analysis on PMMA-OTFT parameter



# Figure Captions

## Chapter 3

- Fig. 3-1 The cross-section of PMMA-OTFT device.
- Fig. 3-2 The optical image of PMMA-OTFT.
- Fig. 3-3 The experimental diagram of probing stage with a light source.

## Chapter 4

- Fig. 4-1 The SEM images of PMMA films rotated at 2000 to 6000 RPM are shown in Fig. (a), Fig. (b), and Fig. (c), respectively. The thickness values are about 450, 300, 200 nm, respectively.
- Fig. 4-2 The capacitance of the Au/PMMA/Pd/Ni MIM structure as a function of the gate voltage at different rotated speed.
- Fig. 4-3 The leakage current of the Au/PMMA/Pd/Ni MIM structure as a function of the electric field at different rotated speed.
- Fig. 4-4 The summary of the capacitance and leakage current at different rotated speed are shown in Fig. (a) and Fig. (b).
- Fig. 4-5 The atomic force microscope (AFM) image of untreated and UV-treated PMMA dielectric film are shown in Fig. (a) and Fig.(b).
- Fig. 4-6 The transfer characteristics of OTFT with untreated PMMA dielectric and UV-treated dielectric are shown in Fig. (a) and Fig. (b).
- Fig. 4-7 The transfer characteristics and the plot of square root of drain current versus the gate voltage with untreated PMMA dielectric under light-illumination and light-off are shown in Fig. (a) and Fig. (b).

- Fig. 4-8 The transfer characteristics and the plot of square root of drain current versus the gate voltage with UV-treated PMMA dielectric under light-illumination and light-off are shown in Fig. (a) and Fig. (b).
- Fig. 4-9 Photo responsivity is plotted as a function of gate-voltage of the untreated and UV-treated OTFT (illumination time is 40s~1000s) are shown in Fig. (a) and Fig. (b).
- Fig. 4-10 The experimental data and the fitting-curves of threshold voltage shift is plotted as a function of time, when the PMMA-OTFTs are illuminated with light and the light-illumination is turn off are shown in Fig. (a) and Fig. (b).
- Fig. 4-11 The X-ray diffraction (XRD) curves of pentacene film on untreated PMMA dielectric and UV-treated PMMA dielectric are shown in Fig. (a) and Fig. (b).
- Fig. 4-12 The Raman spectrum of pentacene film on untreated PMMA dielectric and UV-treated PMMA dielectric are shown in Fig. (a), Fig. (b), Fig. (c) and Fig. (d).
- Fig. 4-13 The plot of leakage current versus time with untreated PMMA dielectric and UV-treated dielectric are shown in Fig. (a) and Fig. (b).
- Fig. 4-14 The band-diagram of UV-treated PMMA OTFT with the process of electron and hole generate and recombine with internal electric field under light-illumination and light-off are shown in Fig. (a), Fig. (b), Fig. (c) and Fig. (d).
- Fig. 4-15 Saturation time-constant and recovering time-constant of UV-treated PMMA-OTFTs and untreated PMMA-OTFTs is plotted as a function of gate voltage, respectively. are shown in Fig. (a) and Fig. (b).

# Chapter 1

## Introduction

### 1-1 Introduction of Organic Thin Film Transistors (OTFTs)

The utilization of organic or polymer materials as a semiconductors layer is realized at the 1980s [1,2]. Owing to the low fabrication-cost, large area, flexibility, the organic thin film transistors (OTFTs) had drawn a lot of interest in the field of display and flexible electronics. In these years, the OTFTs performance has been improved and comparable to the hydrogenated amorphous silicon transistors (a-Si:H TFT) [3]. To fabricate organic transistors on glass or flexible substrates, it is essential to lower down the thin-film deposition temperature. A suitable gate dielectric is a major obstacle that must be overcome. Many researchers propose novel methods to lower down the deposition temperature, such as by using the sputtering or spin-on process. The silicon dioxide ( $\text{SiO}_2$ ) gate-insulator needs to be deposited at high-temperature in vacuum. This high-temperature process is not suitable for plastic substrate, which are commonly used for flexible electronics. Therefore, the OTFTs can be fabricate at low-temperature ( $<100^\circ\text{C}$ ). Among the low temperature process, organic insulators such as poly(4-vinylphenol), poly(methyl methacrylate) and photo-aligned polyimide have been demonstrated on flexible

substrate [4,5]. Due to the potential for electronic device applications, such as various sensors [6,7,8] so how to make a high responsivity sensors is a issue to improve.

## 1-2 Spin-on Coated Dielectrics

Inorganic dielectrics such as thermally-grown silicon dioxide ( $\text{SiO}_2$ ) or silicon nitride ( $\text{SiN}_x$ ), are the most gate-dielectrics for Si-based electronics. However, for organic electronics on large-area or flexible devices, the inorganic dielectrics are not suitable. One concern may be the deposition-temperature, and other may be the interface properties between the organic/dielectric films. It is also well suggested that the interaction of  $\pi$ -conjugated pentacene to the gate dielectric surfaces, will strongly affect the growth and determine the morphology of the organic film [9]. With the use of organic or polymer dielectrics, the defects and grain boundaries in the pentacene film will be reduced. As a result, pentacene-OTFTs with polymer or organic dielectrics show high field-effect mobility in PVP gate-dielectric [10], polyimide gate-dielectric [11] and PMMA gate-dielectric [12]. As summarized in Table I. Hence, new dielectrics such as organic or polymeric materials, which can be spin-coated and dip-coated at low-temperature, will be more suitable to organic electronics.

### **1-3 Applications of Organic Transistors to Optical Devices**

In recent years, a number of groups have demonstrated the use of polymer or organic-based devices as the photo-detectors. These detectors can be classified into two main groups: the two-terminal photodiode and the three-terminal phototransistor. Photodiode is a semiconductor device with a P-N junction, but the phototransistor has higher sensitivity than that in photodiode. Besides, phototransistor has a good on/off switch properties. In recent years, phototransistors have been realized on organic transistor. For the applications on optoelectronic, it is important to understand the effects of light-illumination on device performance, as well as the underlying physics.



### **1-4 Motivation**

Our goal is to fabricate organic and low-temperature OTFTs as the photo sensors. We also present the UV-treatment on the surface of PMMA film to improve photo responsivity. Consequently, we try to investigate the effects of UV-light treatment on PMMA gate-dielectric. Finally, we propose an assumption to discuss what is the dominated factor to influence these difference in OTFT properties.

## 1-5 Thesis Organization

In Chapter 1, we introduce the back-ground of OTFTs, spin-on coated dielectrics, and motivation of the thesis. In Chapter 2, we introduce the transportation mechanisms of organic semiconductor, photonic excitation and response on organic devices, and parameter extraction. In Chapter 3, the fabrication and the structure of OTFTs are presented. In Chapter 4, electrical properties of PMMA dielectric, effects of UV-treatment on PMMA dielectric, and effects of light-illumination on PMMA-OTFTs are discussed. Finally, we make a conclusion in Chapter 5.



# Chapter 2

## Theoretical Background of OTFTs

### 2-1 Introduction

OTFTs are based on the conjugated polymers, oligoacenes, or fused aromatics. Most of these organic or polymer semiconductors are p-type material. Recently, many molecular semiconductors, such as pentacene, thiophene oligomers, and regioregular poly(3-alkyl-thiophene) are proposed. The pentacene ( $C_{22}H_{14}$ ) is a promising candidate for future electronic devices and an interesting model system, due to its superior field effect mobility and environmental stability [13].



### 2-2 Transportation Mechanisms of Organic Semiconductor

Carrier transportation in the organic semiconductors have been investigated on the theory and modeling in the past years [14]. Organic conductors are conjugated materials, where the  $\pi$ -electrons are conducted intra the molecular. Its crystalline is formed by relatively weak Van der Waals interaction between molecules, where the molecular-stacking determines the carrier transportation. Hence, the carrier transport is described by different models than the covalent-bonded semiconductors. In covalent-bonded semiconductors, carriers move as highly delocalized plane waves in



wide bands and have a very high mobility. But in weak-bonded organic semiconductors, the high-mobility model is no longer valid.

Recently, two principal types of theoretical model are used to describe the transport in organic semiconductors : “The band-transport model” and “The hopping models”. However, band transport may not suit for some disordered organic semiconductors, in which carrier transport is govern by the hopping between localized states. Hopping is assisted by phonons and the mobility increases with temperature. Typically, the mobility is very low, usually much lower than  $1\text{cm}^2/\text{V}\cdot\text{sec}$ . The boundary between “band transport” and “hopping” is divided by materials mobilities ( $\sim 1\text{cm}^2/\text{V}\cdot\text{sec}$ ) at room-temperature (RT) [15]. Many kinds of polycrystalline organic semiconductors , such as several members of the acene series including pentacene, rubrene, have RT mobility over the boundary [16]. Sometimes, temperature-independent mobility was found in some polycrystalline pentacene devices [17]. Thus, this observation argued that the simply thermal activated hopping process governed the whole carrier transport behaviors in high quality polycrystalline pentacene film, despite that the temperature independent mobility has been observed in exceptional cases [18].

Organic thin-film transistors (OTFTs) based on conjugated polymers or small molecules have been widely studied over the last ten years. A specific feature of

OTFTs is that the material is solvable and can be fabricated that a low-cost. For instance, the process of inject-printing or screen-printing will also be available [19,20].

When polymeric or organic materials are used as semiconductor layers in OTFTs, the surface-energy difference between semiconductor layer and gate-dielectric will be an important issue [21]. For instance, the surface energy will influence the crystalline ordering, morphology, and structure drastically [22].

On the other hand, function groups on gate-dielectrics will also play an important role to the OTFT performance and characteristics. It is reported that the UV irradiation on polymers will change the functional groups. The UV-light irradiation will lead to a dissociative excitation of C-C or C-H bonds in the polymer dielectric layer. It has also been demonstrated that the UV-light irradiation on PMMA films in air results in the formation of  $-COH$  as well as  $-COOH$  functional end group [23]. Additionally, it has also been identified that the UV-light irradiation on polymer dielectric may result in carrier traps at interface [24]. Base on these researches, the UV-light irradiation on PMMA films should influence the properties of carrier transport in pentacene-OTFT.

## 2-3 Photonic excitation on organic devices

The well-proposed theory of photo-generated-carrier in organic or polymers semiconductors is the exciton model. Photons with a proper energy, which is larger than the band-gap, will be absorbed in the semiconductor. As a result, absorbed photons will create excitons (bound electron-hole pairs). After a very short meanwhile, these excitons will dissociate into electrons and holes. Some of the photo-generated holes maybe are trapped that contribute to the large initial negative threshold voltage, thereby reducing the threshold voltage. The absorption and luminescence in organic materials can be studied by the spectra. The properties of absorption and luminescence are explained by molecular orbital. The electronic structure of organic or polymeric material follows the “Pauli exclusion principle”, electrons begin to fill up from the lowest energy level will get a lowest energy electron configuration. When electrons only fill up at highest occupied molecular orbital (HOMO), this molecular state is at the ground state. When the electron is excited to anti-bonding orbital state, it is called as the excitation state. Then, the excited electrons release to lower energy level, e.g. the “triplet excited state”, and luminescence to ground state. This luminescence light is named as phosphorescence. On the other hand, the excited electrons release to “singlet excited-state”, and directly luminescence to ground state, is named as fluorescence. The process-time of

phosphorescence and fluorescence is about millisecond and nanosecond, respectively.

Several probable processes of photo-generated carrier in organic semiconductor are summarized as:

1. Directly, band-to-band excitation
2. Exciton formation and subsequent dissociation (electric field, surface, or impurity induced) into free carrier.

1. Electric field makes the exciton dissociation to electron and hole, electron move toward positive voltage direction, hole move toward opposite direction.

2. If the surface have a trap and insulator have impurity, these two trap site will trap electron and hole.

3. Photo-injection of carriers from the metal source/drain electrodes into the semiconductor.

4. De-trapping of carriers trapped in localized gap states in the semiconductor

In organic devices, the applied-voltage will build up electric-field, which effects the diffusion or the drift of photo-generated-carriers. For instant, in an organic field-effect transistor (OFET), the gate-voltage and the drain-voltage can drive the carriers. It is also known that in most OFETs, which are p-type and operated in accumulated-mode. The negative gate-voltage ( $V_G < 0$ ) and drain-voltage ( $V_D < 0$ )

will force the photo-generated holes move toward the interface of semiconductor/gate-dielectric and drain-electrodes, respectively.

The photo-generated holes will be collected by the drain-electrodes and result in a higher drain-current. The excess drain-current is usually defined as the photo-generated current and described as:

$$I_{photo} = I_{Drain,illum} - I_{Drain,dark}$$

$I_{Drain,illum}$  is the drain-current under illumination,  $I_{Drain,dark}$  is the drain-current in dark, and the difference between  $I_{Drain,illum}$  and  $I_{Drain,dark}$  is defined as the photo-current  $I_{photo}$ .



Actually, only a portion of incident photons will be converted to the excitons and contribute to photo-current. To quantify the ratio between the photo-current and the incident photons, the quantum efficiency (QE:  $\eta$ ) is usually used. It can be express as:

$$\eta = \frac{I_{photo} / e}{P_0 / h\nu}$$

As described,  $I_{photo}$  is the photo-current,  $e$  is the electronic charge,  $P_0$  is the incident light-power,  $h$  is the Planck's constant, and  $\nu$  is the incident light-wavelength. In general, quantum efficiency is also described the ratio of generated electron-hole pairs over the incident photon numbers.

As for the photo-detector, the responsivity ( $R$ ) is used to estimate the detector performance. The responsivity is deduced from quantum efficiency and can be expressed as:

$$R = \frac{I_{photo}}{P} = \frac{I_{photo}}{(P_0/A) \cdot W \cdot L}$$

Where  $P$  is the normalized incident power on device,  $A$  is the light spot-size,  $W$  is device channel width, and  $L$  is device channel length. The responsivity is usually a function of wavelength, and also named as “spectral responsivity” or “radiant sensitivity”.

## 2-4 Parameter Extraction



In this section, the methods of extraction the mobility, the threshold voltage, the subthreshold swing, the maximum interface trap density, and the is characterized, respectively.

### 2-4-1 Field-effect Mobility ( $\mu_{eff}$ )

Generally, the linear mobility (for  $V_D < V_G - V_{th}$ ) can be extracted from the transconductance maximum  $g_m$  in the linear region:

$$g_m = \left[ \frac{\partial I_D}{\partial V_G} \right]_{V_D = \text{const}} = \frac{WC_{ox}}{L} \mu V_D \quad (2.5)$$

The saturation mobility (for  $V_D > V_G - V_{th}$ ) can also be extracted from the slope

of the curve in the squared drain-current versus the gate-voltage diagram:

$$\sqrt{I_D} = \sqrt{\frac{W}{2L} \mu C_{ox} (V_G - V_{TH})} \quad (2.6)$$

#### 2-4-2 Threshold voltage ( $V_{th}$ )

We extract the threshold voltage from equation (2.6), the intersection point of the squared drain-current versus gate-voltage.

#### 2-4-3 Subthreshold swing ( $S.S.$ ) and Interface trap-density ( $N_{it}$ )

Subthreshold swing is also important characteristics for device application. Its is a factor to estimate how rapidly the device switches from the off state to the on state in the region of exponential current increase. It is defined by:

$$S = \left. \frac{\partial V_G}{\partial (\log I_D)} \right|_{V_D = \text{constant}}, \text{ when } V_G < V_T \text{ for p-type.}$$

moverover, the subthreshold swing also represents the interface quality and the defect density [26], the maximum interface state trap-density can be extracted by :

$$N_{it} = \left[ \frac{S \cdot \log(e)}{kT / q} - 1 \right] \cdot \frac{C_i}{q}$$

a high-performance TFTs will show a low subthreshold swing.

#### 2-4-4 Responsivity ( $R$ )

In a photodetector, the ratio of the electrical output to the optical input. Responsivity is usually expressed in amperes per watt, or volts per watt, of incident radiant power. The responsivity is deduced from quantum efficiency and can be expressed as:

$$R = \frac{I_{photo}}{P} = \frac{I_{photo}}{(P_0 / A) \cdot W \cdot L}$$

Where  $P$  is the normalized incident power on device,  $A$  is the light spot-size,  $W$  is device channel width, and  $L$  is device channel length. The responsivity is usually a function of wavelength, and also named as “spectral responsivity” or “radiant sensitivity”.





# Chapter 3

## Experiments

### 3-1 PMMA-Dielectric Fabrication and UV-light Treatment

A glass substrate was rinsed in the (KG detergent) and de-ionized water in an ultrasonic system before the device fabrication. Consequently, a 10Å Ni layer and a 200Å Pd layer were deposited as gate electrodes. PMMA [poly(methyl methacrylate)] we used was obtained from MicroChem Corp (with a molecular weight of 95000), which was dissolved in anisole at 95 wt %. The PMMA was then spun onto the gate electrodes at a speed about 4000 to 5000rpm. After spin-on coating, the PMMA was transferred to a hot-plate and annealed at 90°C for 30minutes. The thickness of PMMA was estimated by the cross-section image of the scanning electron microscopy (SEM) and capacitance measurement, respectively.

After the dielectric fabrication, a portion of PMMA dielectrics were chosen to expose to the UV-light in ambient atmosphere about 60-90sec. The UV-light we used was with an output power 40mW and a wavelength around 175-285nm.

### 3-2 PMMA-OTFTs Fabrication

The devices we used in experiments are the inverted-stacked structure with top-contact source/drain electrodes. The detail fabrication processes are as follows:

### Step1. Substrate and gate electrode

As mentioned in PMMA dielectric fabrication, the substrate we used was glass and the gate electrodes was Pd/Ni (thickness:200Å/10Å) bi-layer, which was deposited by the thermally-coated vacuum system under the pressure around  $3 \times 10^{-6}$  torr.

### Step2. Gate dielectric formation

The dielectric we used was thermally-solidified PMMA film and its thickness was about 300nm-400nm. A portion of the PMMA film was also exposed to the UV-light about 60-90sec.



### Step3. Pentacene film deposition

The pentacene material obtained from Aldrich without any purification was directly used for the deposition. The deposition of pentacene film is started at a pressure around  $1 \times 10^{-6}$  torr. The deposition-rate is controlled at  $\sim 0.5 \text{ \AA}/\text{sec}$  and the thickness of pentacene film was about 100nm, monitored by the quartz crystal oscillator. The pentacene film region is defined through the shadow-mask and the substrate temperature is controlled at  $70^\circ\text{C}$  during the pentacene film deposition.

#### Step4. Source/Drain deposition

A 100nm Au layer is deposited as the source/drain electrodes on the pentacene film. Through the shadow-mask, the OTFT channel width and length is defined as  $100\ \mu\text{m}$  and  $1000\ \mu\text{m}$ , respectively. The PMMA-OTFT structure and the optical image are also shown in Fig.3-2.

In this study, all the experimental data were obtained from the semiconductor parameter analyzer (HP 4156A) and impedance analyzer (HP 4284) in the dark at room temperature.

### 3-3 Photonic excitation



To study the effects of light-illumination on PMMA-OTFTs, we setup a probing stage with a light-source, which is shown in Fig.3-3. The light-source we used in the experiment is a 150W halogen lamp, which is filtered at 460nm by a band-pass filter with a full width half maximum (FWHM) about 10nm. The filtered-light is guided by an optical fiber and focused by a microscope. The total light power and the spot diameter on the probing stage was about  $1.5\text{-}2.7\ \mu\text{W}$  and 2.5mm, respectively. The light power we used in the experiment is measured by the Newport 1815-C.

# Chapter 4

## Result and Discussion


### 4-1 Electrical properties of PMMA dielectric

#### 4-1-1 Fabrication of PMMA dielectrics and relative dielectric properties

To fabricate a suitable capacitance for OTFTs, the dielectric thickness, roughness, and leakage-current are important demands. In this experiment, we try to adjust the rotational speed of spin-on process to control the dielectric thickness. In Fig. 4-1(a), (b), (c), we show the scanning electron microscope (SEM) images of PMMA dielectrics on gate-electrode with different rotational speed. When the rotational speed is increase from 2000 raid per minute (RPM) to 6000RPM, the PMMA thickness will reduce from 500nm to 250nm. To further obtain the capacitance values, all the PMMA dielectrics with different thickness are fabricated as the metal-insulator-metal (MIM) structures for capacitance measurement. The measured capacitance values from the impedance analyzer (Agilent 4284) indicate that the capacitance will increase from 4nF/cm<sup>2</sup> to 9.3nF/cm<sup>2</sup> when the rotational speed increase from 2000RPM to 6000RPM. The result is agreed with the estimate dielectric thickness in SEM image and plotted as a capacitance-voltage (C-V) diagram in Fig. 4-2. Additionally, we also measure the leakage-current density from these

MIM structure. The leakage-current curves are plotted as a function of gate-voltage in Fig. 4-3. As we can observe, the dielectric leakage is as low as  $3 \times 10^{-9} \text{ A/cm}^2$  when the rotational speed remain lower than 5000RPM. When the rotational speed is larger than 5000RPM, the dielectric leakage increases drastically to the level about  $10^{-6} \text{ A/cm}^2$ . Therefore, if we consider a low-leakage PMMA dielectric with maximum capacitance in this experiment, the rotational speed about 4000-5000RPM should be the optimized value. All the C-V and leakage-current measurement are summarized in Fig. 4-4(a) and (b), respectively.

#### 4-1-2 UV- treatment on PMMA dielectric



We try to use the UV-treatment to change the functional groups on PMMA. In the reported studies, it indicates that the UV-treatment on PMMA will result in the formation of  $-COH$  as well as  $-COOH$  groups [23]. Besides, it is also reported that the UV-treatment will create charged-sites on the polymer dielectrics and result in the change of OTFT characteristics. In our experiment, the exposed time of PMMA dielectric is about 60-90sec. The AFM images of untreated PMMA and UV-treated PMMA is shown in Fig. 4-5(a) and (b), respectively. It reveals that the PMMA roughness is not changed and remains around 0.2-0.3nm as well. Further more, we also measure the capacitance value and the leakage-current. As summarized in Table

II, the capacitance of untreated PMMA and UV-treated PMMA dielectric is 8.4nF/cm<sup>2</sup> and 8.6nF/cm<sup>2</sup>, respectively. The leakage-current density at 1MV/cm is  $3.4 \times 10^{-9}$  A/cm<sup>2</sup> for untreated PMMA dielectric and  $3.6 \times 10^{-9}$  A/cm<sup>2</sup> for UV-treated PMMA dielectric. It is evident that the UV-treatment on PMMA will not change its surface and dielectric properties significantly.

#### **4-2 Characteristics of OTFTs with distinct PMMA-dielectrics**

In Fig. 4-6(a) and (b), we show the transfer characteristics of OTFT with untreated PMMA dielectric and UV-treated dielectric, respectively. In OTFT with untreated PMMA dielectric, the device shows a mobility about 0.24cm<sup>2</sup>/v-sec, a threshold voltage about -6.8V, and a subthreshold swing about 0.9 V/decade. On the other hand, the OTFT with UV-treated dielectric show a similar mobility about 0.21cm<sup>2</sup>/v-sec, a lower threshold voltage about -3.3V, and a larger subthreshold swing about 1.8 V/decade. It is interesting that with the UV-treatment on dielectric, the threshold voltage will be reduced and the subthreshold will be increased. But the mobility almost remains unchanged. Further more, we try to estimate the trap-density at the pentacene /PMMA interface from the subthreshold swing method. It is found that the interface trap density is about  $7.42 \times 10^{11}$  at untreated PMMA interface and  $1.64 \times 10^{12}$  at UV-treated PMMA interface. The result indicates that the

UV-treatment on PMMA dielectric will create additional trap-sites. Besides, from the change of threshold voltage, it implies that these UV-created sites may act as the charged sites and influence the carrier concentration in OTFT channel region.

### **4-3 Characteristics of light-illumination on PMMA-OTFTs**

In Fig. 4-7(a) and (b), we show the transfer characteristics of OTFT with untreated PMMA dielectric under light-illumination. It reveals that turn-on current increases and the threshold voltage shifts toward more positive values after the OTFT is exposed to illumination. With the illumination-time increase up to about 1000 seconds, the threshold voltage shift ( $\Delta V_{th}$ ) reaches a value about 2V, and the drain-current will increase from  $9.96 \times 10^{-7} \text{A}$  to  $1.39 \times 10^{-6} \text{A}$ . In Fig. 4-8(a) and (b), we also show the transfer characteristics of OTFT with UV-treated PMMA dielectric under light-illumination. Similar to the aforementioned results, the threshold voltage will shift positively and the drain-current will increase after light-illumination. However, in OTFT with UV-treated PMMA dielectric, the threshold voltage shift ( $\Delta V_{th}$ ) approaches a larger value about 4V and the drain-current will increase from  $1.09 \times 10^{-6} \text{A}$  to  $1.57 \times 10^{-6} \text{A}$ . We also try to estimate the photo responsivity of the OTFTs and plot the curves as a function of gate-voltage in Fig. 4-9(a) and 4-9(b). As we can see, the initial value of photo responsivity (after light-illumination about 40

seconds) of untreated-PMMA OTFT and UV-treated-PMMA OTFT is about 4.5A/W and 6A/W, respectively. When the illumination time approaches 1000 seconds, the photo responsivity is about 9A/W (in untreated-PMMA) and 11A/W (in UV-treated PMMA). It is evident that PMMA-OTFT will show a larger photo responsivity when the PMMA-dielectric is treated by the UV-light.

#### **4-4 Time-dependent parameter analysis on PMMA-OTFTs under and after light-illumination**

Evidently, the mobility remains almost unchanged otherwise the light-illumination is turned on and turned off. The subthreshold swing will slightly increase under illumination and reduce to its original values, which is due to the extraction method. Some studies indicate it is not significantly affected by the illumination but an artifact, because the illumination will not change the density of states in organic film [25]. The threshold voltage in UV-treated PMMA-OTFTs will shift positively and rapidly about 2.7V and approach a saturated-value about 3.7V when the illumination time is closed to 1000seconds. However, when the illumination is turned off, the threshold voltage will return to its original value slowly. On the other hand, the untreated PMMA-OTFTs show a smaller threshold shift about 0.9V and reach a saturated-value about 1.2V when the illumination time is closed to



1000seconds. To quantify the time-dependent threshold voltage shift ( $\Delta V_{th}$ ), we try to use the double exponential equation to describe the threshold voltage shift as a function of time:

$$\Delta V_{th}(t) = V_1 \cdot (1 - e^{-\frac{t}{\tau_1}}) + V_2 \cdot (1 - e^{-\frac{t}{\tau_2}}) \quad \text{under light-illumination}$$

$$\Delta V_{th}(t) = V_1' \cdot e^{-\frac{t}{\tau_1'}} + V_2' \cdot e^{-\frac{t}{\tau_2'}} \quad \text{illumination turned-off}$$

Where the  $V_1$ ,  $V_2$ ,  $V_1'$ , and  $V_2'$  are the fitting parameters;  $\tau_1$  and  $\tau_2$  present the “saturation time-constant” of threshold shift under light-illumination;  $\tau_1'$ , and  $\tau_2'$  present the “recovering time-constant” of threshold voltage after illumination is turned off. The experimental data and the fitting-curves are plotted in Fig. 4-10(a) and Fig.4-10(b) all the correspondent fitting parameters and time-constants are summarized in Table III. As we can observe, two distinct time-constants can be sufficient to fit the experimental data very well. One exhibits a rapid but minor reaction with a shorter time-constant; the other exhibits a slow but major reaction with a longer time-time constant. We compare the “saturation time-constants” of  $\Delta V_{th}$  between untreated and UV-treated PMMA-OTFTs under illumination. It is found that two OTFTs show similar shorter time-constants ( $\tau_1$ ) around 30-40 seconds, but show different longer time-constant ( $\tau_2$ ) about 581 seconds for UV-treated PMMA-OTFTs and 1001 seconds for untreated PMMA-OTFTs. We conclude that the UV-treated PMMA-OTFTs will show a larger  $\Delta V_{th}$  and shorter saturation

time-constant than that in untreated PMMA-OTFTs. On the other hand, both OTFTs exhibit a shorter “recovering time-constants” ( $\tau_1'$ ) about 50-60 seconds. The longer “recovering time-constants” ( $\tau_2'$ ) is about 712 seconds in untreated PMMA-OTFTs. However, in UV-treated PMMA-OTFTs, the  $\tau_2'$  is prolonged to 3687 seconds. It is also conclude that the UV-treated PMMA-OTFTs show a smaller  $\Delta V_{th}$  recovering and a longer recovering time-constant than that in untreated PMMA-OTFTs.

#### 4-5 Material analysis on PMMA-OTFTs

Since the characteristics and response are much different in untreated and UV-treated OTFTs, it is important to deduce the effects from UV-treatment. The dielectric properties are almost the same, so we try to investigate the pentacene film properties on different PMMA dielectric firstly. In Fig. 4-11(a) and Fig. 4-11(b), we show the x-ray diffraction (XRD) curves of pentacene film on untreated and UV-treated PMMA dielectrics. Both pentacene films show the (001) signal with a peak value about  $5.73^\circ$  (degree) and a FWHM about  $0.06^\circ$  (degree). The higher order signal of (002) and (003) peak is also observed with a values about  $11.46^\circ$  (degree) and  $17.21^\circ$  (degree), respectively. According to the XRD analysis, it implies that the pentacene films on untreated and UV-treated PMMA dielectrics are almost identical. The UV-treatment on PMMA dielectric seems not effect the

pentacene crystal significantly. Consequently, we also try to verify the pentacene film by the Raman spectrum. With the Raman analysis, the conformational transition during carrier transport [26]. The pentacene vibration-modes of  $C-H$  (around 1155-1179 $\text{cm}^{-1}$ ) and  $C-C$  (around 1353-1380 $\text{cm}^{-1}$ ) bindings are plotted in Fig. 4-12(a) and (b) (from pentacene on untreated PMMA dielectric); (c) and (d) (from pentacene on UV-treated PMMA dielectric). Both pentacene film show the similar Raman shifts at 1158 $\text{cm}^{-1}$ , 1179  $\text{cm}^{-1}$ , 1153  $\text{cm}^{-1}$ , and 1173  $\text{cm}^{-1}$ . The result also reveals that the intermolecular coupling will not be changed even if the pentacene film is deposited on untreated or UV-treated PMMA dielectric. Finally, we also show the absorption spectrum of the two pentacene films on different PMMA dielectrics. Once again, two pentacene film have almost identical absorption properties. Base on these material analyses, the crystalline, molecular coupling, and the absorptive properties of pentacene film on these distinct PMMA dielectrics should be almost identical.

In order to verify the property of dielectric trapping, we try to observe the time-dependent leakage current on these two PMMA dielectrics. It had been investigated that when the dielectric trapping appears in the gate-insulator. The leakage-current will be a function of time and approach to a saturated value when the measurement time is long enough. In Fig. 4-13 (a) and (b), we show the

time-dependent leakage-current of untreated and UV-treated PMMA, respectively. It is evident that both leakage-currents are almost kept at a constant level about  $2 \times 10^{-9}$  A/cm<sup>2</sup> and will not change with time, even if these dielectrics are stress at a reversed gate bias-stress about -20V. Hence, we conclude that the dielectric trapping is not significant in these two PMMA dielectrics.

#### **4-6 Plausible origin of the enhancement on photo responsivity**

The material analyses have shown that the pentacene film and the dielectric properties are almost alike in these two PMMA-OTFTs. It is probable the differences of OTFT transfer characteristic and its photo responsivity are originate from the interface traps, which are created by the UV-light treatment. These UV-created interface traps should be act as negative sites, which may withdraw the electrons but accumulate the holes in pentacene film, near the interface of pentacene and PMMA dielectrics (UV-treated). Hence, the hole-accumulation will result in an upward-banded HOMO-band and build up an internal electric field near the interface. When the PMMA-OTFTs are illuminated, the electron-hole pairs will be generated in the pentacene film. In UV-treated PMMA-OTFTs with build-in electric field, holes will be swept toward the PMMA-dielectric and the electrons will be swept toward bulk of pentacene. The process assisted with an additional build-in electric field will

come about faster than the case in untreated PMMA-OTFTs. Interestingly, from the analysis of saturation time-constant, the UV-treated PMMA-OTFTs show a smaller total saturation time than the untreated PMMA-OTFTs. It reveals that the process of threshold-voltage shift is faster in the UV-treated PMMA OTFTs. The result is good agreed with the assumption. Consequently, if the light-irradiation is removed, the electrons and holes begin to recombine. In the UV-treated PMMA-OTFTs, with a build-in electric field, the spatial separation between electrons and holes will be longer than that in untreated PMMA-OTFTs. As a result, the recombination rate will be reduced and show a prolonged recovering time. Therefore, we deduced from the recovering time-constant. Significantly, the total recovery time-constant is longer in UV-treated PMMA OTFTs than that in untreated PMMA OTFTs. Again, the result is good agreed to the proposed model. The correspondent model can be explained by the band-diagram and plotted in Fig. 4-14 (a), (b), (c), and (d). Furthermore, to verify the proposed assumption, we try to extract the saturation time-constant and the recovering time-constant of photo-generated current, as a function of gate-voltage.

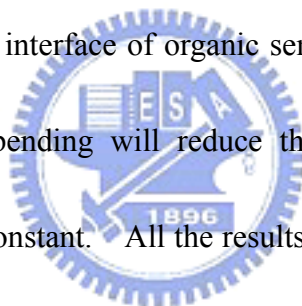
The extraction equation is identical to the time-dependent threshold voltage shift:

$$I_{photo}(t) = I_1 \cdot (1 - e^{-\frac{t}{\tau_1}}) + I_2 \cdot (1 - e^{-\frac{t}{\tau_2}}) \quad \text{under light-illumination}$$

$$I_{photo}(t) = I_1' \cdot e^{-\frac{t}{\tau_1}} + I_2' \cdot e^{-\frac{t}{\tau_2}} \quad \text{illumination turned-off}$$

Where the  $I_1$ ,  $I_2$ ,  $I_1'$ , and  $I_2'$  are the fitting parameters;  $\tau_1$  and  $\tau_2$  present

the “saturation time-constant” of threshold shift under light-illumination;  $\tau_1'$ , and  $\tau_2'$  present the “recovering time-constant” of threshold voltage after illumination is turned off. In Fig. 4-15(a) is the Saturation time-constant as a function of gate voltage. When the gate voltage increase,  $\tau_1$  is almost the same but  $\tau_2$  will decrease in untreated and UV-treated PMMA-OTFTs. In Fig.4-15(b) is Recovering time-constant as a function of gate voltage. When the gate voltage increase,  $\tau_1'$  is almost the same but  $\tau_2'$  will increase in untreated and UV-treated PMMA-OTFTs. Since the higher gate-voltage will produce larger band bending and increase the internal electric field near the interface of organic semiconductor and gate-dielectric. Evidently, a larger upward bending will reduce the saturation time-constant and prolong the recovering time-constant. All the results are agreed with the assumption of build-in electric field. Base on these experimental results, we may conclude that the UV-treated PMMA, which may create additional interface traps, should be the origin of these distinct responses in PMMA-OTFTs. The proposed “build-in electric field” model should be a suitable explanation to the observed results.



# Chapter 5

## Conclusion

### 5-1 Conclusion

In this study, we try to fabricate the OTFTs with solution-based PMMA gate-dielectrics and investigate the effects of UV-light treatment on PMMA gate-dielectrics. With the UV-light treatment, the threshold voltage and the subthreshold swing will be significantly altered, but the field-effect mobility remains almost unchanged. When the light-irradiation on these OTFTs, the devices with UV-light treatment will show a larger threshold voltage shift and a larger photo responsivity than those devices without UV-light treatment. In order to investigate the effect of UV-light treatment on OTFTs characteristics, the material analysis and the dielectric leakage-current measurement are proceeded. It is found that the variation of the semiconductor layer and the trapping in the dielectric layer should not be the dominated factors. By the time-dependent analysis of threshold voltage shift and photo-generated current, the saturated time and the recovering time show a strong correlation to the gate-voltage. That implies the electric-field in the organic semiconductor film will influence the behavior drastically. It is most probably the UV-light treatment may create the charged traps at the interface of the

PMMA-dielectric and the organic semiconductor, which will result in a build-in electric-field in the organic semiconductor near the PMMA gate-dielectric. Hence, the OTFTs with UV-light treatment will show different characteristics, such as a faster saturation time and a longer recovering time.





## References

- [1] A. Tsumura, K. Koezuka, and T. Ando, "Macromolecular electronic devices: Field-effect transistor with a polythiophene thin film", *Appl. Phys. Lett.* vol.49, pp. 1210, (1986).
- [2] J. H. Burroughes, C. A. Jones, and R. H. Friend, "Polymer diodes and transistors: new semiconductor device physics", *Nature*, vol. 335, pp.137, (1988).
- [3] Y. Y. Lin, D. J. Gundlach, S. F. Nelson, and T. N. Jackson, "Pentacene organic thin-film transistors-molecular ordering and mobility", *IEEE Electron Device Lett.* vol. 18, pp. 87, (1997).
- [4] H. Sirringhaus, R. J. Wilson and R. H. Friend, " Mobility enhancement in conjugated polymer field-effect transistors through chain alignment in a liquid-crystalline phase", *Appl. Phys. Lett.* Vol.77, pp.406, (2000).
- [5] W. Y. Chou, and H. L. Cheng, "An Orientation-Controlled Pentacene Film Aligned by Photoaligned Polyimide for Organic Thin-Film Transistor Applications", *Adv. Funct. Mater.* , vol. 14, pp. 811, (2004).
- [6] Tobat P. I. Saragi, Robert Pudzich, Thomas Fuhrmann-Lieker, and Josef Salbeck, "Ultraviolet-sensitive field-effect transistor utilized amorphous thin films of organic donor/acceptor dyad", *Appl. Phys. Lett.*, vol. 90, pp. 143514, (2007).
- [7] Zheng-Tao Zhu, Jeffrey T. Mason, Rüdiger Dieckmann, and George G. Malliaras, "Humidity sensors based on pentacene thin-film transistors", *Appl. Phys. Lett.*, vol. 81, pp. 4643, (2002).
- [8] Jeong-M. Choi, Jiyoul Lee, D. K. Hwang, Jae Hoon Kim, and Seongil Im, "Comparative study of the photoresponse from tetracene-based and pentacene-based thin-film transistors", *Appl. Phys. Lett.* Vol. 88, pp. 043508,

(2006).

- [9] De Angelis, F.; Toccoli, T.; Pallaoro, A.; Coppedè, N.; Mariucci, L.; Fortunato, G.; Iannotta, S., “SuMBE based organic thin film transistors”, *Synth. Met.*, vol. 146, pp. 291, (2004).
- [10] Hagen Klauk, Marcus Halik, Ute Zschieschang, Günter Schmid, and Wolfgang Radlik, “High-mobility polymer gate dielectric pentacene thin film transistors”, *J. Appl. Phys.*, vol. 92, pp.5259, (2002).
- [11] Yusaku Kato, Shingo Iba, Ryohei Teramoto, Tsuyoshi Sekitani, and Takao Someya, ” High mobility of pentacene field-effect transistors with polyimide gate dielectric layers”, *Appl. Phys. Lett.* , vol.84, pp.3789, (2004).
- [12] F. De Angelis, S. Cipolloni, L. Mariucci, and G. Fortunato, “High-field-effect-mobility pentacene thin-film transistors with polymethylmetacrylate buffer layer”, *Appl. Phys. Lett.*, vol. 86, pp. 203505, (2005).
- [13] Yanming Sun, Yunqi Liu, and Daoben Zhu, “Advances in organic field-effect transistors”, *J. Mater. Chem.*, vol. 15, pp. 53, (2005).
- [14] R. A. Street, D. Knipp, and A. R. Völkel, “Hole transport in polycrystalline pentacene transistors”, *Appl. Phys. Lett.*, vol. 80, pp. 1658, (2002).
- [15] G. Horowitz, “Organic field-effect transistors”, *Adv. Mater.*, vol. 10, pp. 365, (1998).
- [16] Y.-Y. Lin, D. J. Gundlach, S. F. Nelson, and T. N. Jackson, “Stacked pentacene layer organic thin-film transistors with improved characteristics”, *IEEE Electron Device Lett*, vol. 18, pp 606, (2000).
- [17] Y.-Y. Lin, D. J. Gundlach, S. F. Nelson, and T. N. Jackson, “Stacked pentacene layer organic thin-film transistors with improved characteristics”, *IEEE Electron Device Lett*, vol. 18, pp 606, (2000).

- [18] S. F. Nelson, Y.-Y. Lin, D. J. Gundlach, and T. N. Jackson, “Temperature-independent transport in high-mobility pentacene transistors”, *Appl. Phys. Lett.*, vol. 72, pp. 1854, (1998).
- [19] U. Zschieschang, H. Klauk, M. Halik, G. Schmid, C. Dehm, “Flexible Organic Circuits with Printed Gate Electrodes”, *Adv. Mater.*, vol. 15, pp 1147, (2003).
- [20] J. Z. Wang, J. Gu, F. Zenhausern, and H. Sirringhaus, “Low-cost fabrication of submicron all polymer field effect transistors”, *Appl. Phys. Lett.*, vol. 88, pp. 133502, (2006).
- [21] Sang Yoon Kwonwoo, Kwonwoo Shin, and Chan Eon Park, “The Effect of Gate-Dielectric Surface Energy on Pentacene Morphology and Organic Field-Effect Transistor Characteristics”, *Adv. Funct. Mater.*, vol. 15, pp. 1806, (2005).
- [22] Pyo, Kyung Soo; Song, Chung Kun, “The effects of simultaneous treatment of SiO<sub>2</sub> gate and Au electrode with octadecyltrichlorosilane and charge transfer molecules on characteristics of pentacene thin film transistors”, *Thin Solid Film*, vol. 485, pp. 230, (2005).
- [23] A. Torikai, M. Ohno, and K. Fueki, “Photodegradation of Poly(methyl Methacrylate) by Monochromatic Light:Quantum Yield, Effect of Wavelengths, and Light Intensity”, *J.Appl. polym. Sci.*, vol 41, pp. 1023, (1990).
- [24] Lay-Lay Chua, Jana Zaumseil, Jui-Fen Chang, Eric C.-W. Ou, Peter K.-H. Ho, Henning Sirringhaus, Richard H. Friend, “General observation of n-type field-effect behaviour in organic semiconductors”, *Nature.*, vol 434, pp. 194 (2005).

- [25] Hamilton, M.C.; Martin, S.; Kanicki, J., “Thin-film organic polymer phototransistors”, IEEE Trans., vol. 51, pp. 877, (2004).
- [26] Horng-Long Cheng, Yu-Shen Mai, Wei-Yang Chou, and Li-Ren Chang, “Influence of molecular structure and microstructure on device performance of polycrystalline pentacene thin-film transistors”, Appl. Phys. Lett., vol. 90, pp. 171926, (2007).



**Table I** The comparison of the different polymer OTFTs electrical properties

<b>Gate Dielectric</b>	$\mu$ ( $\text{cm}^2/\text{V}\cdot\text{sec}$ )	$V_{\text{TH}}$ (V)	<b>S.S.</b> (V/decade)	<b>On/off</b> <b>Current ratio</b>
<b>Cross-linked PVP</b>	3	-5	1.2	$10^5$
<b>Polyimide</b>	1	Not mention	Not mention	$10^6$
<b>SiO<sub>2</sub>/PMMA</b>	1.4	-12	0.71	$10^6$



**Table II** The comparison of untreated and UV-treated PMMA dielectrics properties

	<b>Capacitance (nF/cm<sup>2</sup>)</b>	<b>Leakage (A/cm<sup>2</sup>) @ 1MV/cm</b>
<b>Untreated</b>	<b>8.43</b>	<b>3.43x10<sup>-9</sup></b>
<b>UV-treated</b>	<b>8.64</b>	<b>3.66x10<sup>-9</sup></b>



**Table III** Time dependent analysis on PMMA-OTFT parameter

**Saturation time constant**

	No UV-treated	UV-treated
V1	0.8758	2.25
V2	0.4845	1.781
$\tau 1$	41.55	32.61
$\tau 2$	1001	581

**Recovering time constant**

	No UV-treated	UV-treated
V1'	0.3502	0.5786
V2'	0.8334	3.149
$\tau 1'$	50.26	65.2
$\tau 2'$	712.5	3687

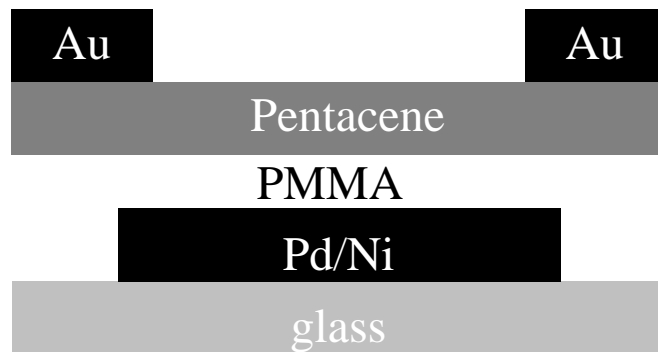


**Fig. 3-1** The cross-section of PMMA-OTFT device.

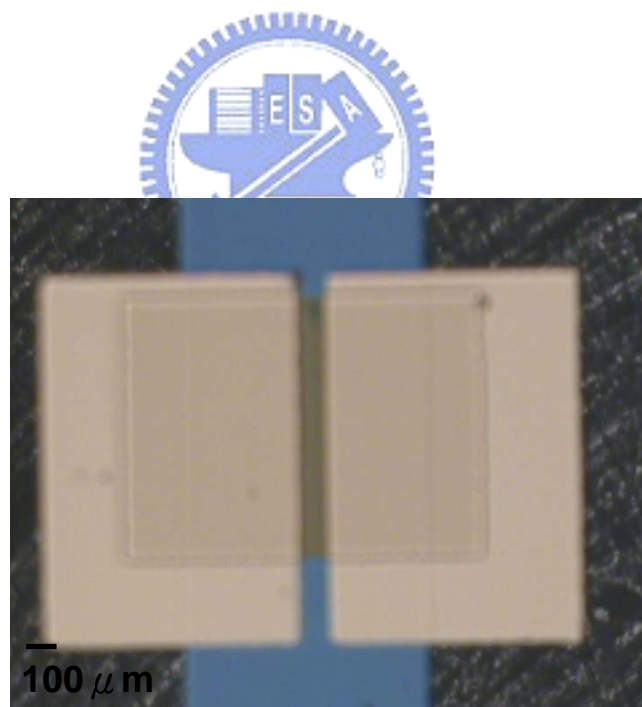


**Fig. 3-2** The optical image of PMMA-OTFT.



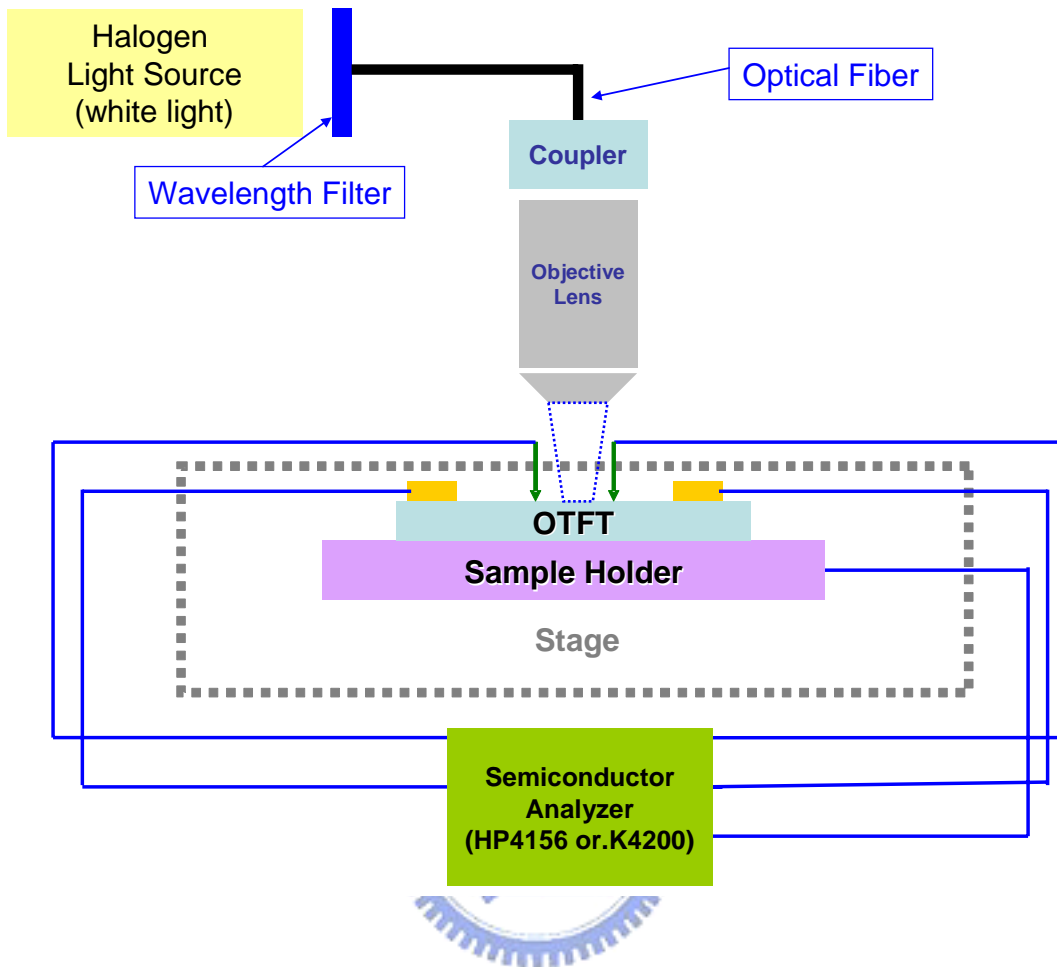


**Fig. 3-3** The experimental diagram of probing stage with a light source.

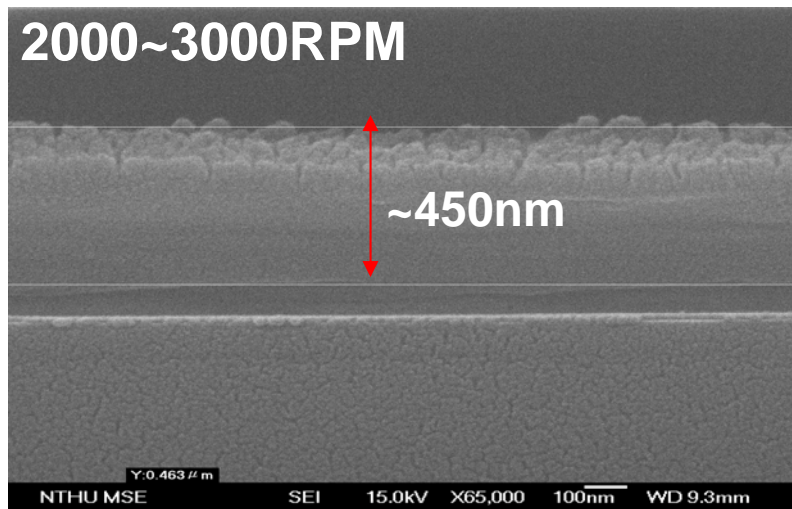


**Fig. 4-1(a)** The scanning electron microscope (SEM) image of PMMA-dielectrics on gate-electrode with a coating speed about 2000-3000RPM.

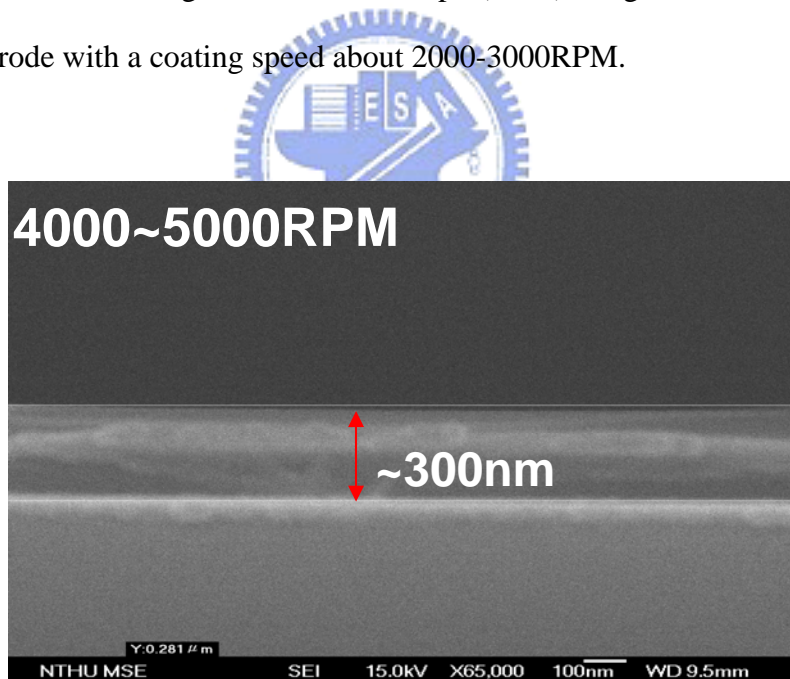


**Fig. 4-1(b)** The scanning electron microscope (SEM) image of PMMA-dielectrics on gate-electrode with a coating speed about 4000-5000RPM.

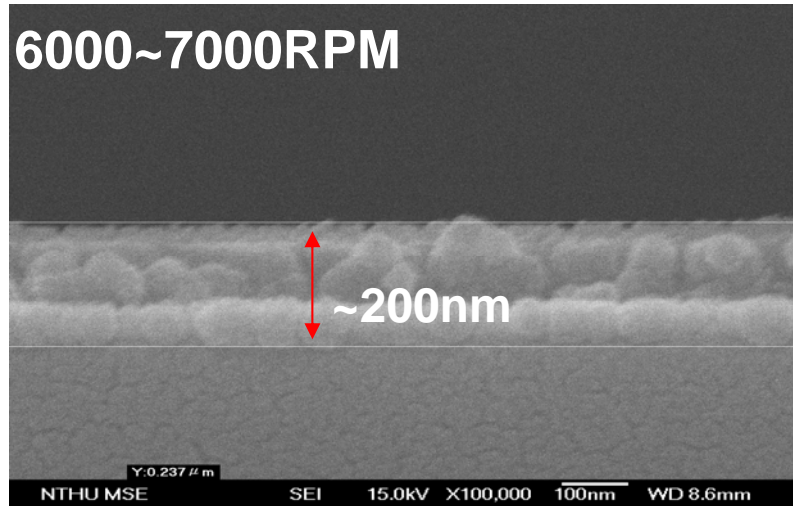


**Fig. 4-1(c)** The scanning electron microscope (SEM) image of PMMA-dielectrics on gate-electrode with a coating speed about 6000-7000RPM.



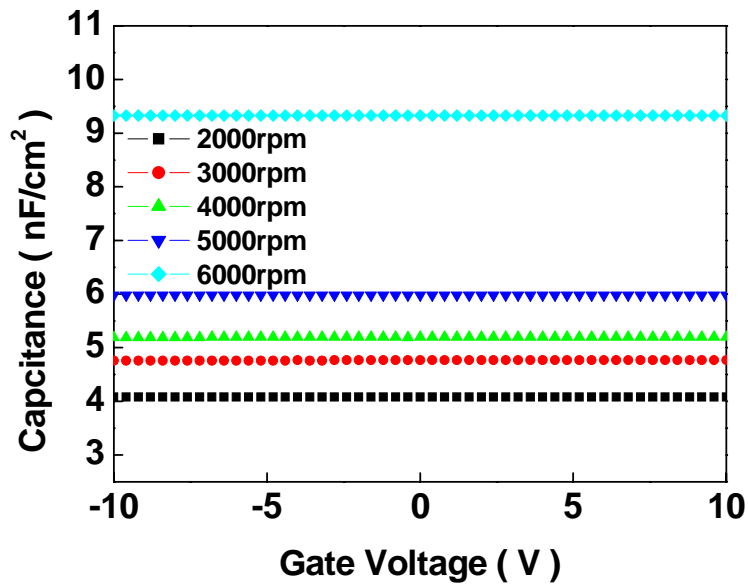


**Fig. 4-2** Capacitance-voltage (C-V) measurement of PMMA-dielectrics with different rotated speed.

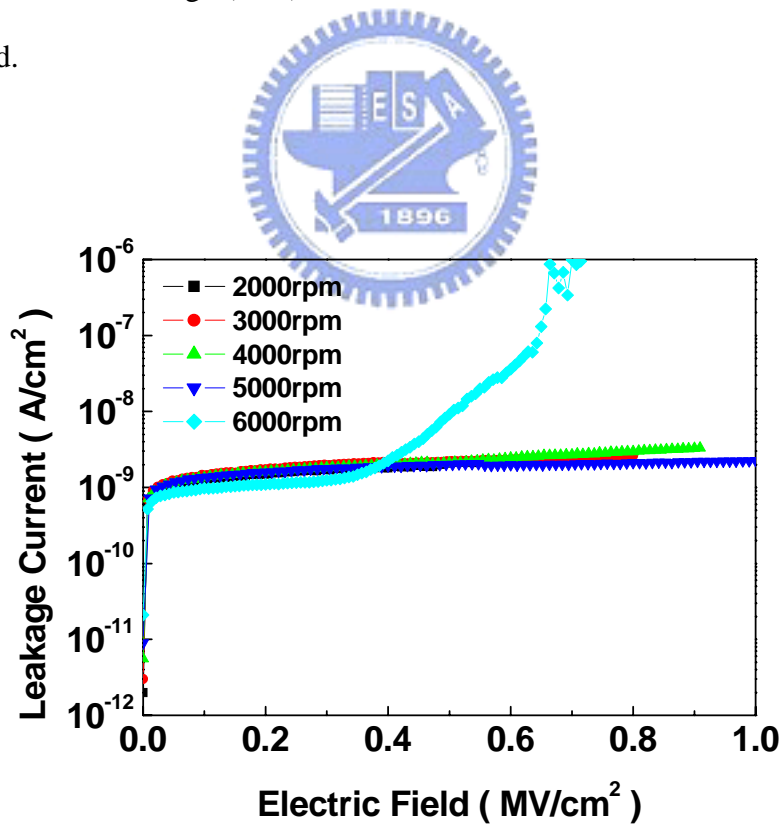


**Fig. 4-3** The leakage-current density versus the electric field (J-E) plot of different PMMA dielectrics, which are fabricated with different rotated speed.

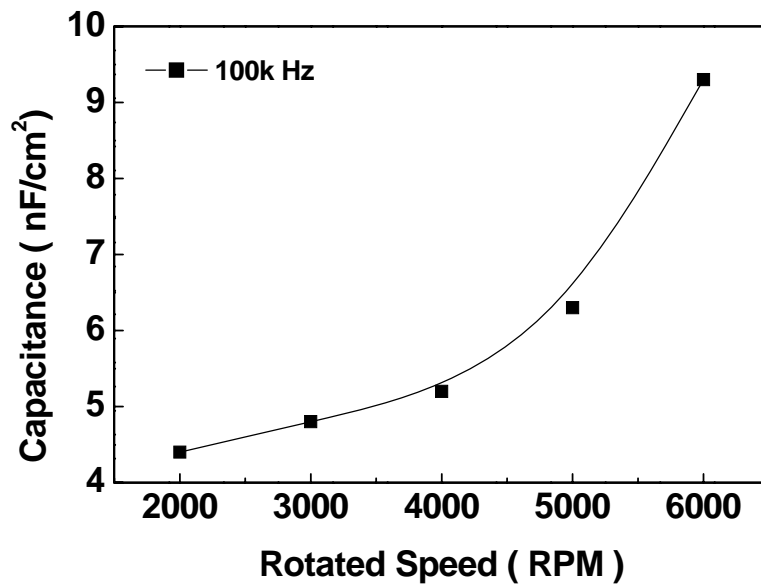


**Fig. 4-4(a)** Capacitance value of PMMA-dielectric is plotted as a function of rotated-speed and measured at a frequency of 100kHz.

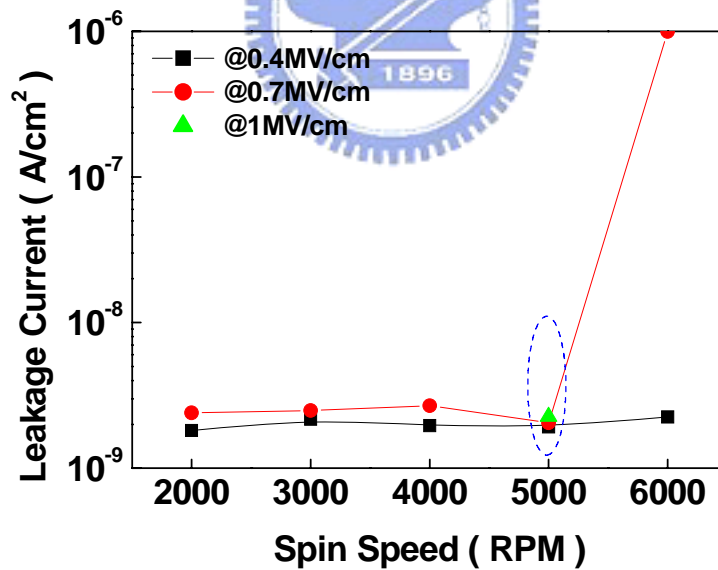


**Fig. 4-4(b)** Leakage-current of PMMA-dielectric is plotted as a function of rotated-speed and measured at different vertical electric field: 0.4MV/cm, 0.7 MV/cm, and 1MV/cm, respectively.

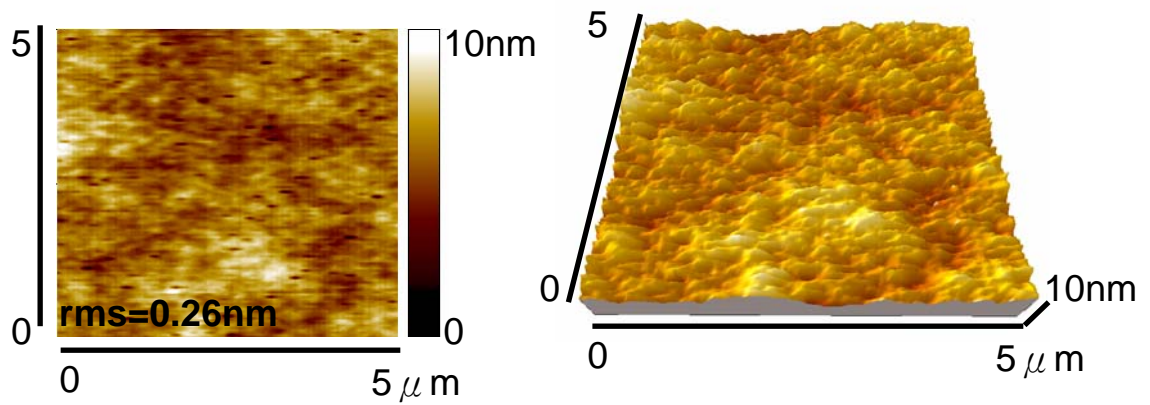


**Fig. 4-5(a)** The atomic force microscope (AFM) images of untreated PMMA dielectric film. The scanning size is fixed to be  $5 \times 5 \mu\text{m}^2$ . The surface roughness is about 0.26nm.

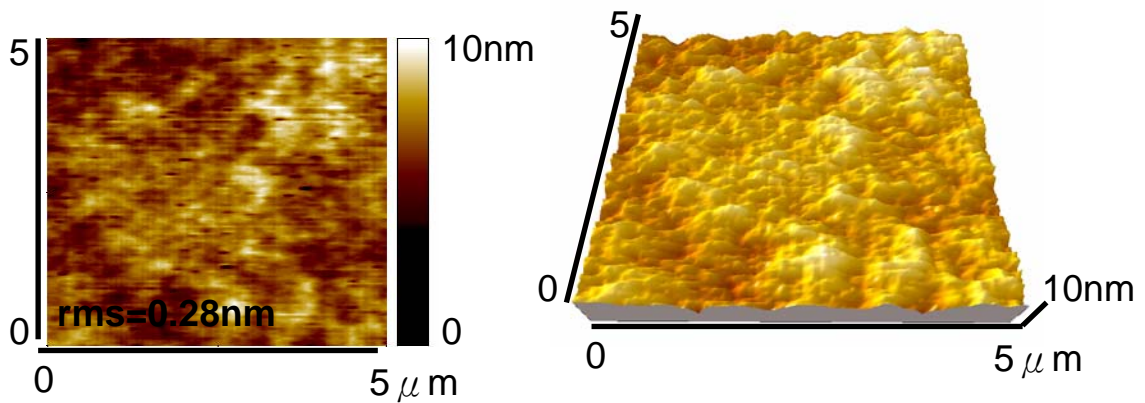


**Fig. 4-5(b)** The atomic force microscope (AFM) image of UV-treated PMMA dielectric film. The scanning size is fixed to be  $5 \times 5 \mu\text{m}^2$ . The surface roughness is about 0.28nm.

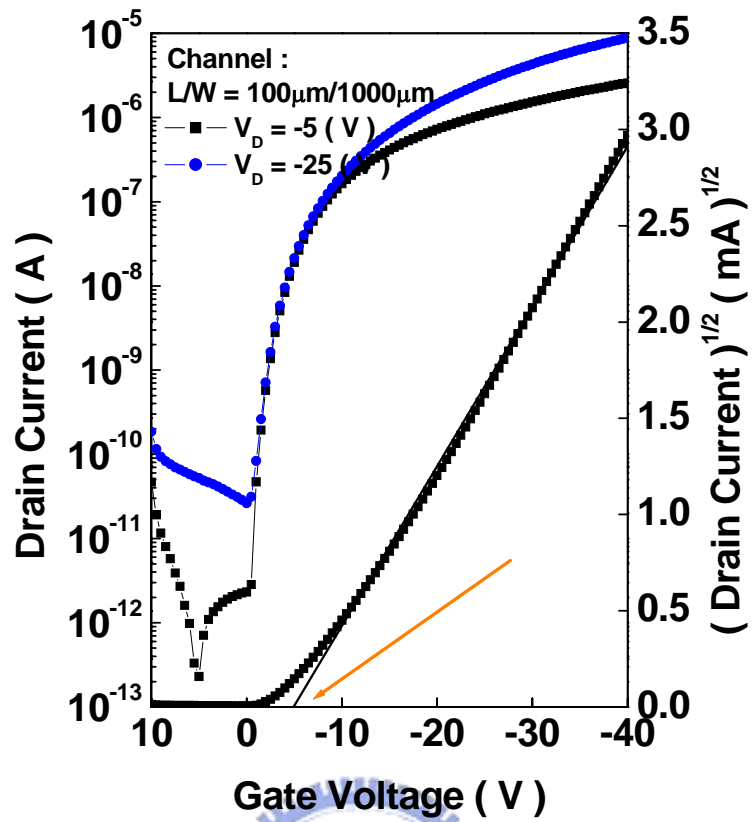


Fig. 4-6(a) Transfer characteristics of OTFT with untreated PMMA dielectric.

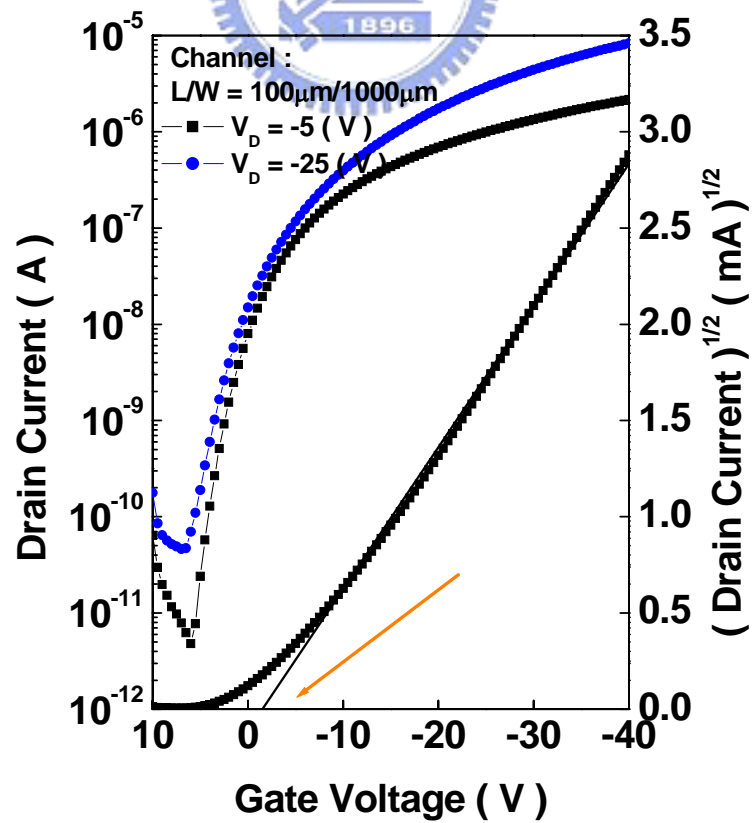
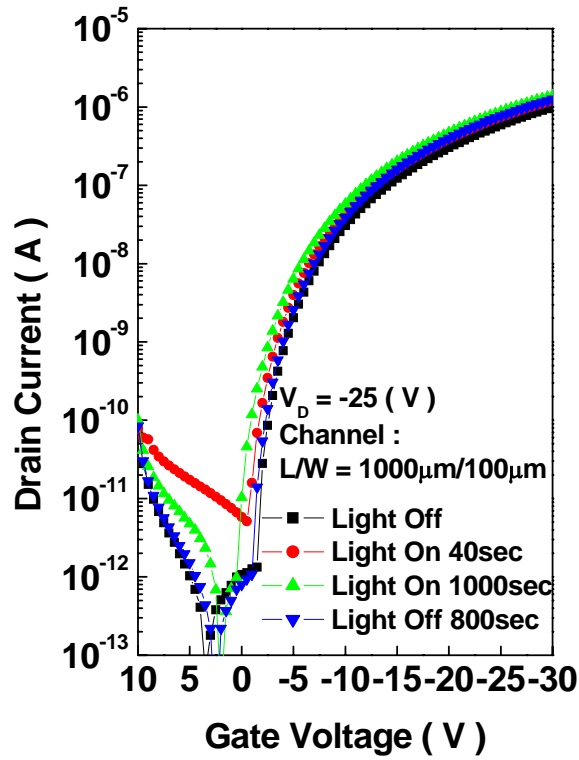
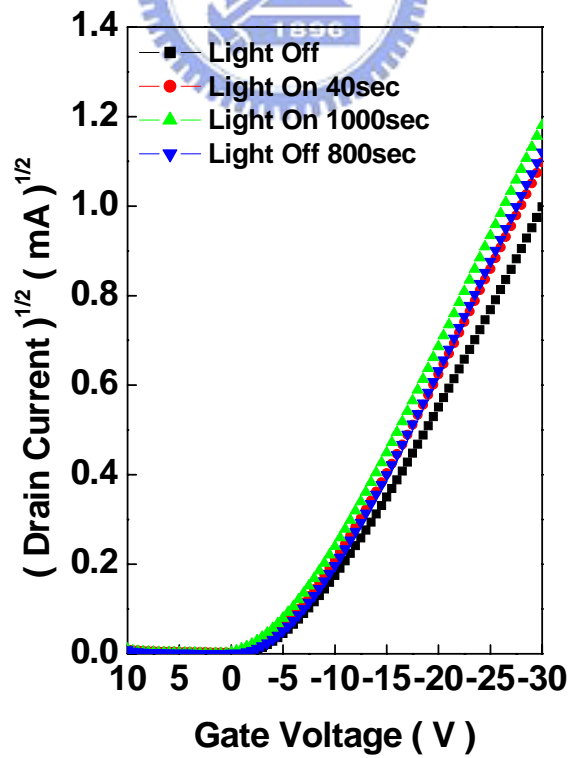


Fig. 4-6(b) Transfer characteristics of OTFT with UV-treated PMMA dielectric.



**Fig. 4-7(a)** The semi-log diagram of transfer characteristics of light-illumination on PMMA-OTFTs (untreated PMMA dielectric).



**Fig.4-7(b)** The linear diagram of transfer characteristics of light-illumination on PMMA-OTFTs (untreated PMMA dielectric).



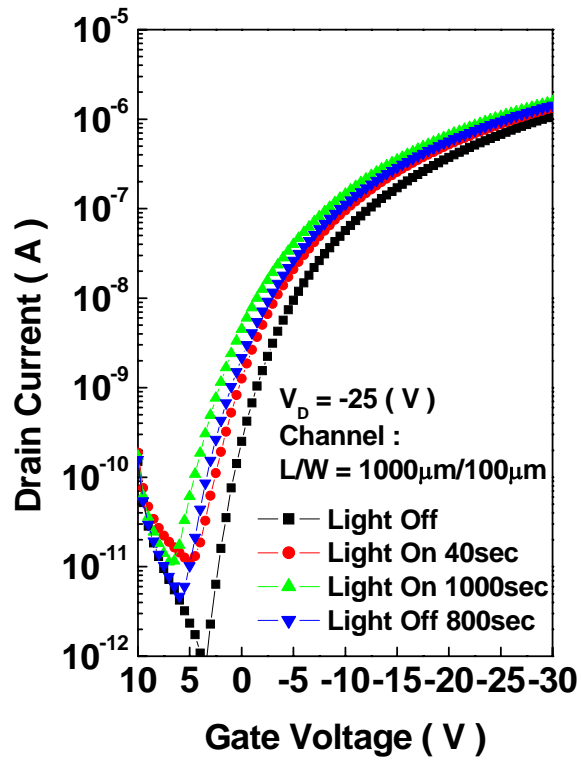


**Fig.4-8(a)** The semi-log diagram of transfer characteristics of light-illumination on PMMA-OTFTs (UV-treated PMMA dielectric).

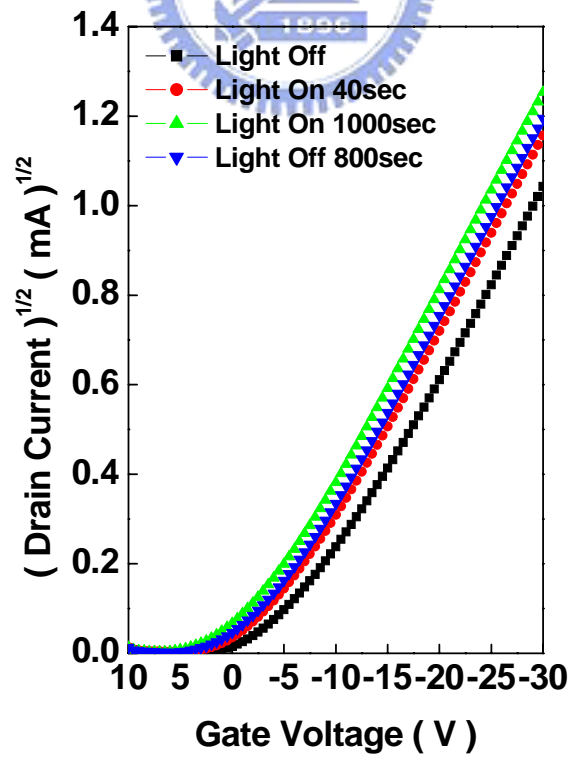


**Fig. 4-8(b)** The linear diagram of transfer characteristics of light-illumination on PMMA-OTFTs (UV-treated PMMA dielectric).

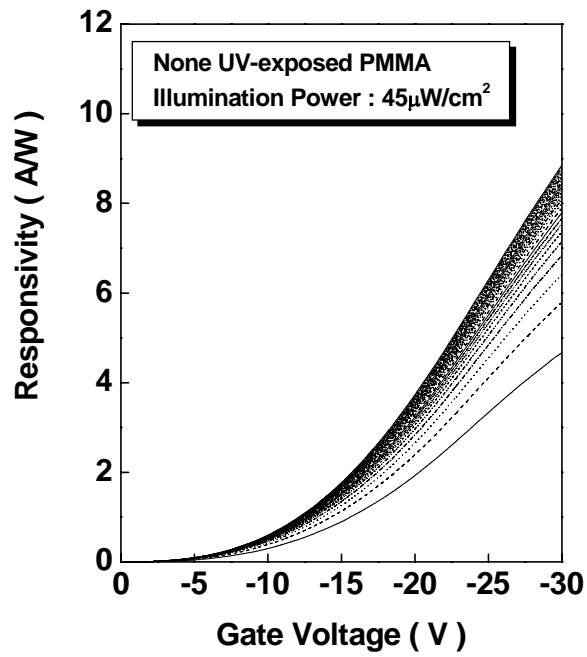


**Fig. 4-9(a)** Photo responsivity is plotted as a function of gate-voltage of the untreated OTFT (illumination time is 40s to1000s).

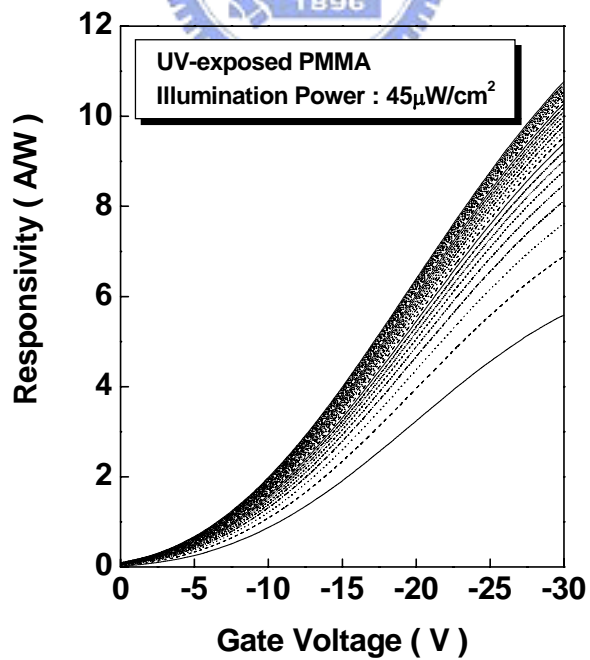


**Fig. 4-9(b)** Photo responsivity is plotted as a function of gate-voltage of the UV-treated OTFT (illumination time is 40s to1000s).

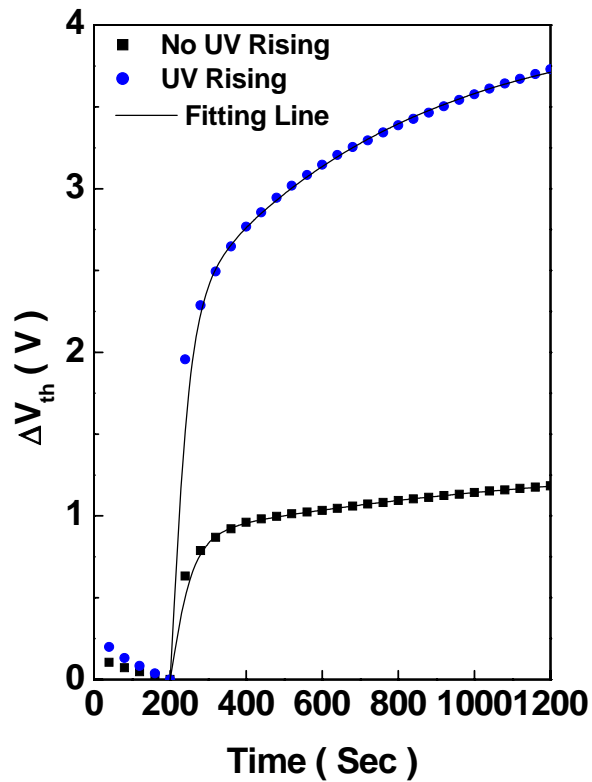


**Fig. 4-10(a)** The experimental data and the fitting-curves of threshold voltage shift is plotted as a function of time, when the PMMA-OTFTs are illuminated with light.

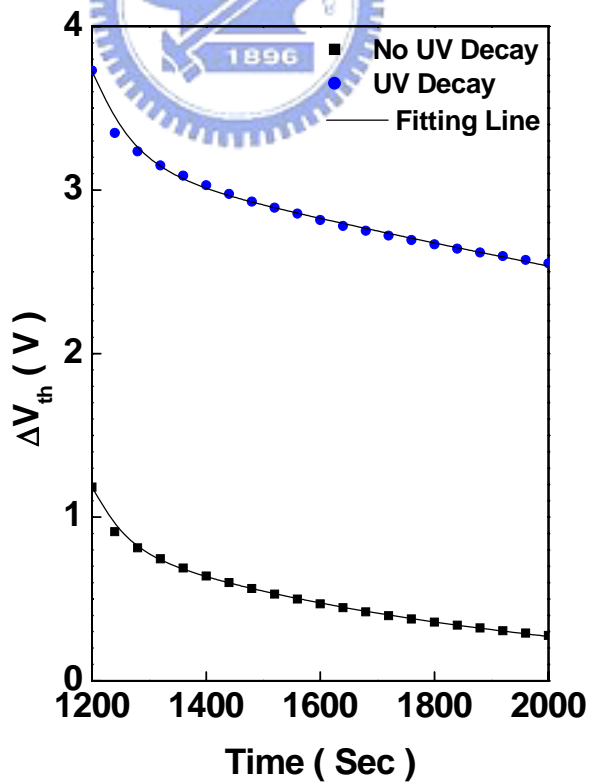


**Fig. 4-10(b)** The experimental data and the fitting-curves of threshold voltage shift is plotted as a function of time, when the light-illumination is turn off.

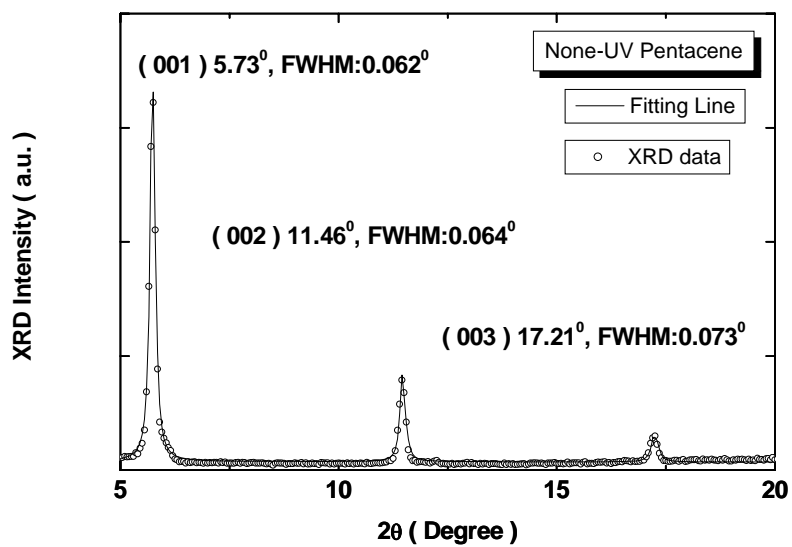


**Fig. 4-11(a)** The X-ray diffraction (XRD) curves of pentacene film on untreated PMMA dielectric.

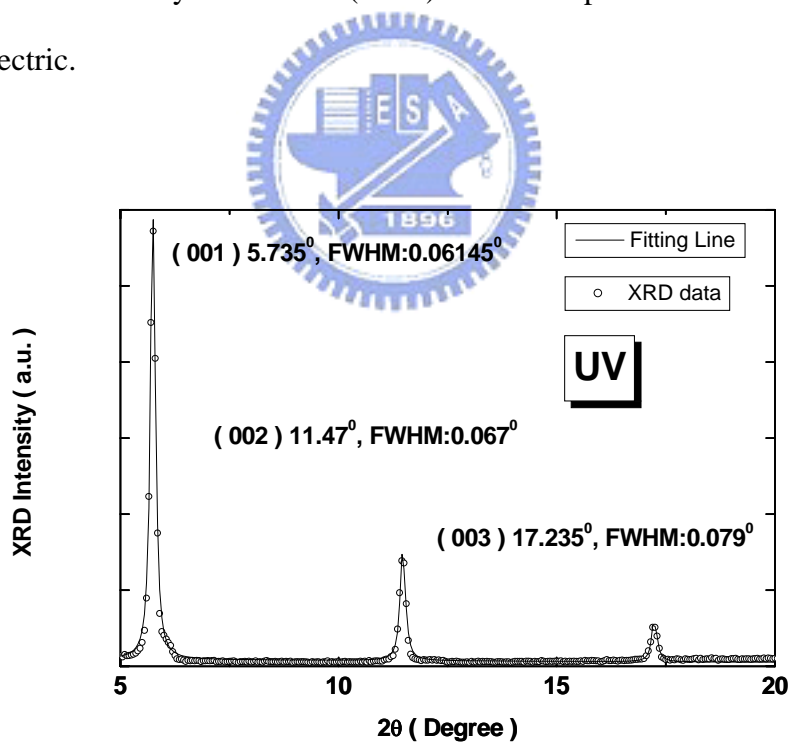


**Fig. 4-11(b)** The X-ray diffraction (XRD) curves of pentacene film on UV-treated PMMA dielectric.

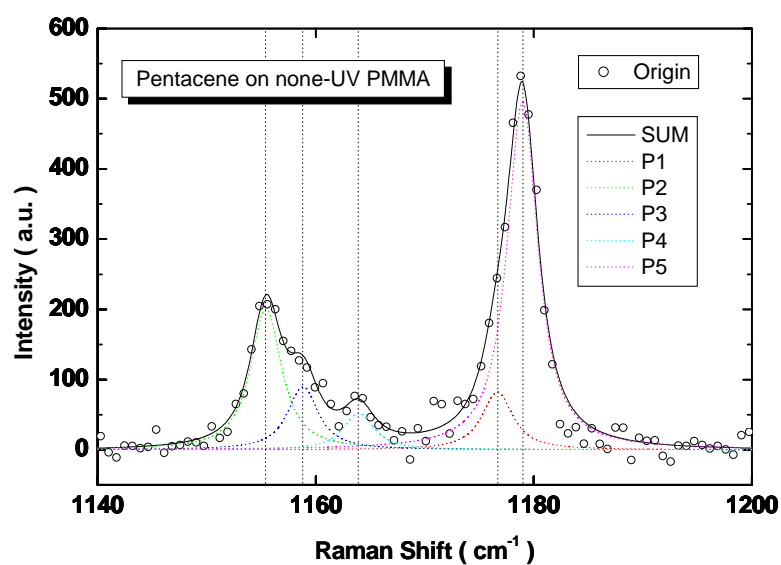


**Fig. 4-12(a)** The Raman spectrum (1140-1200 $\text{cm}^{-1}$ ) of pentacene film on untreated PMMA dielectric.

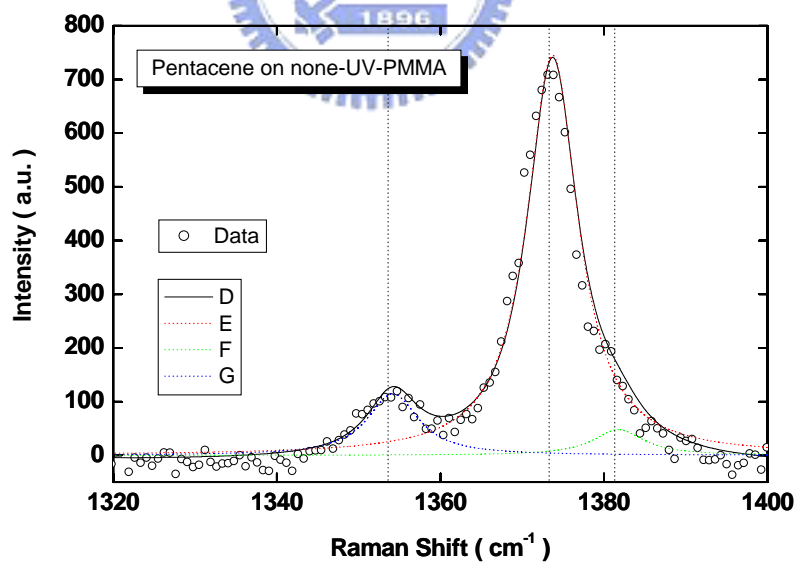


**Fig. 4-12(b)** The Raman spectrum (1320-1400 $\text{cm}^{-1}$ ) of pentacene film on untreated PMMA dielectric.

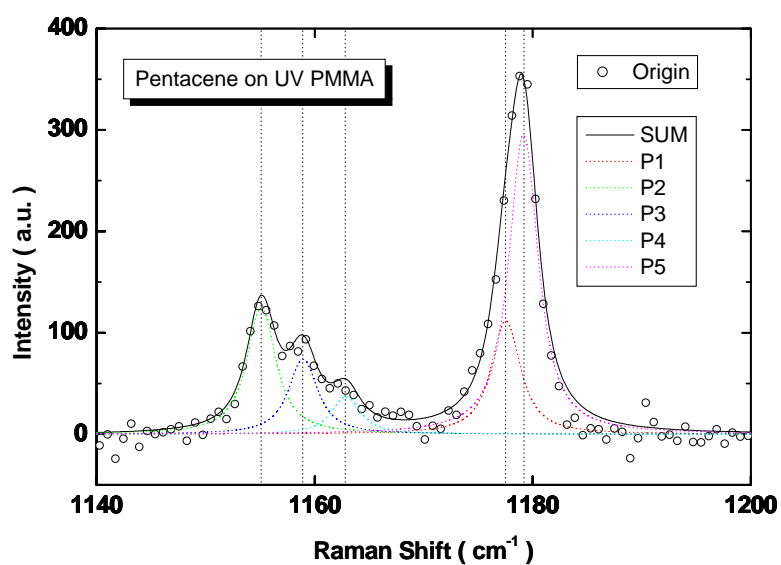


**Fig. 4-12(c)** The Raman spectrum (1140-1200cm<sup>-1</sup>) of pentacene film on UV-treated PMMA dielectric.

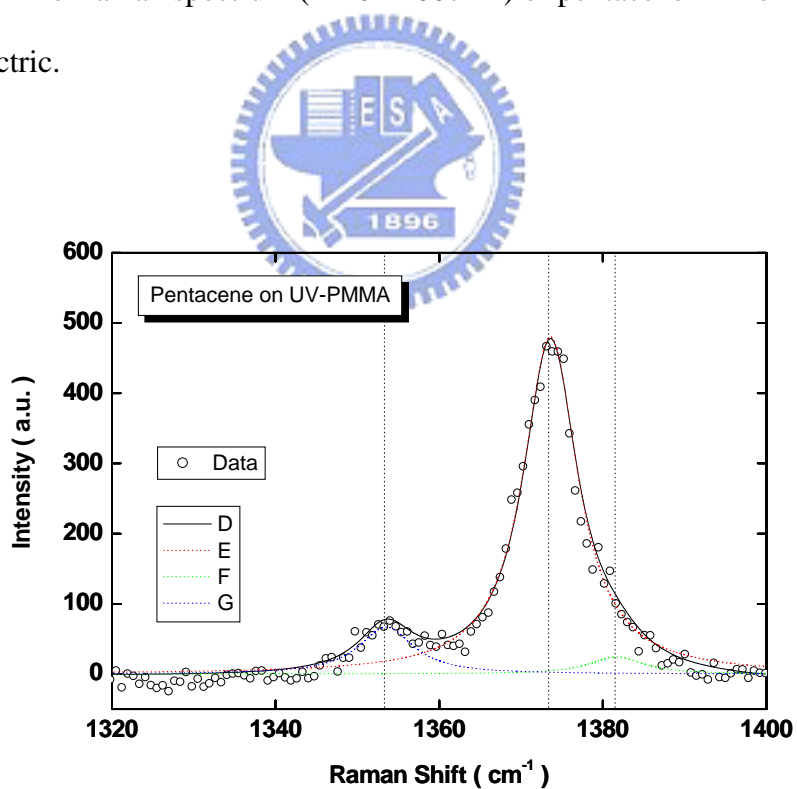


**Fig. 4-12(d)** The Raman spectrum (1320-1400cm<sup>-1</sup>) of pentacene film on UV-treated PMMA dielectric.

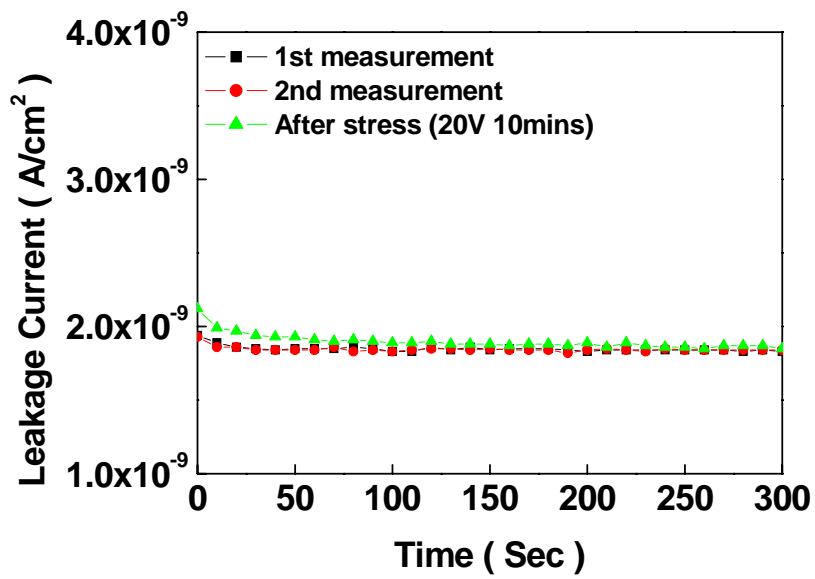


**Fig. 4-13(a)** The leakage-current of untreated PMMA dielectric is plotted as a function of time.

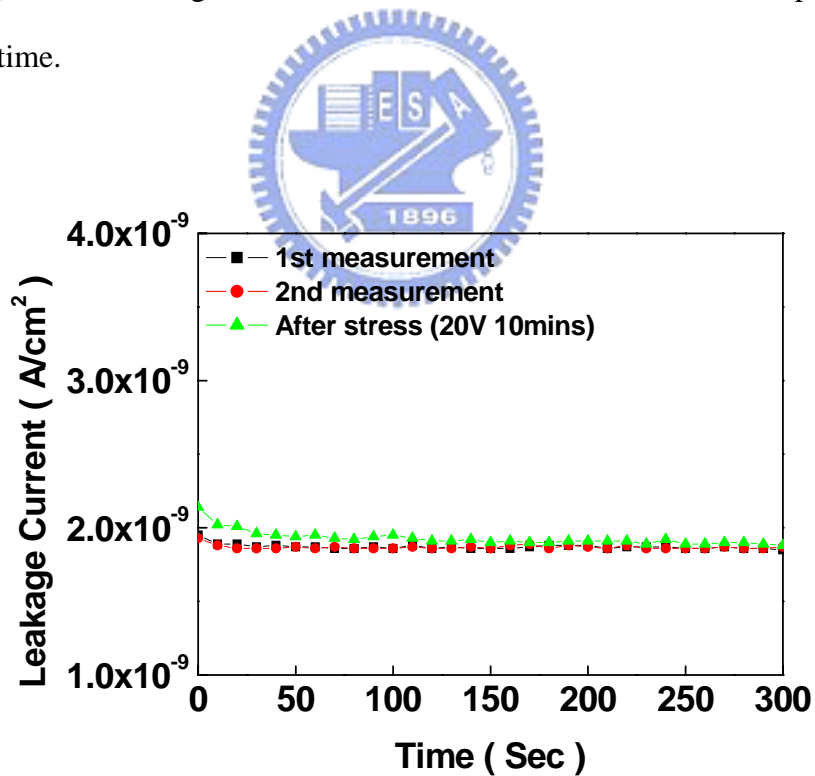


**Fig. 4-13(b)** The leakage-current of UV-treated PMMA dielectric is plotted as a function of time.

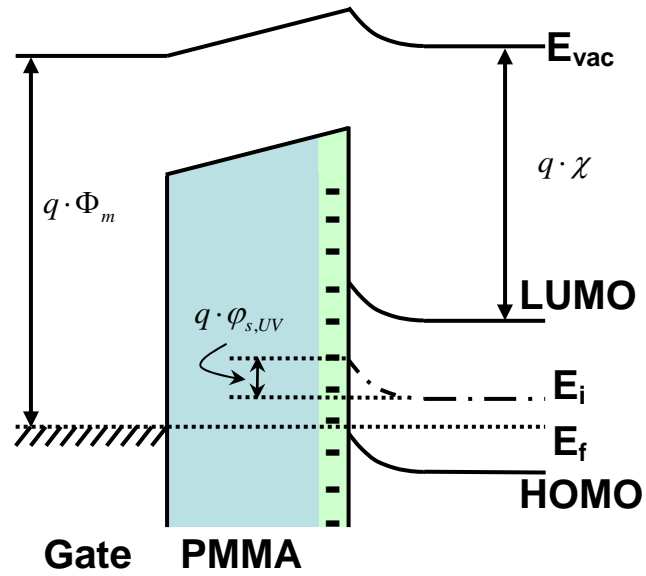


**Fig. 4-14(a)** The band-diagram of UV-treated PMMA OTFT with negative sites, which will result in an additional build-in electric field.

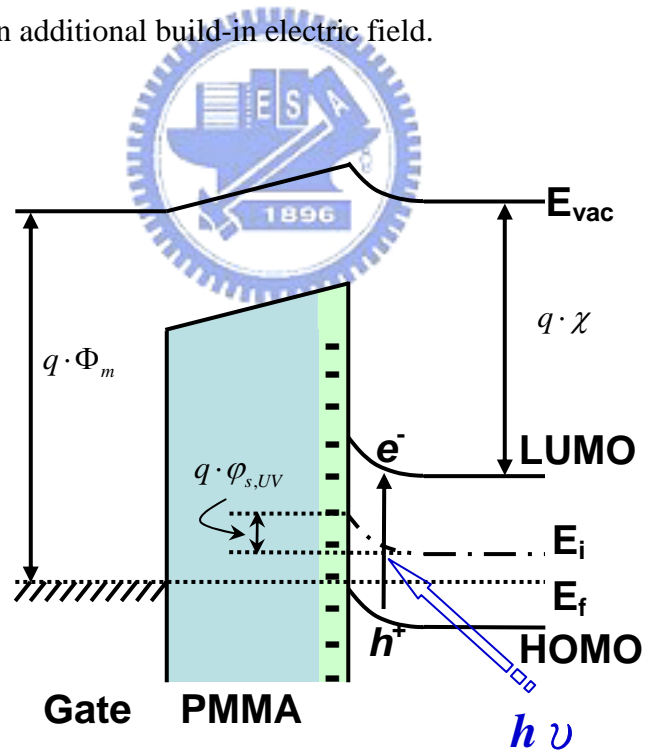


**Fig. 4-14(b)** The UV-treated PMMA OTFT is illuminated with light. The electron-hole pairs will be generated and swept by the build-in electric field.



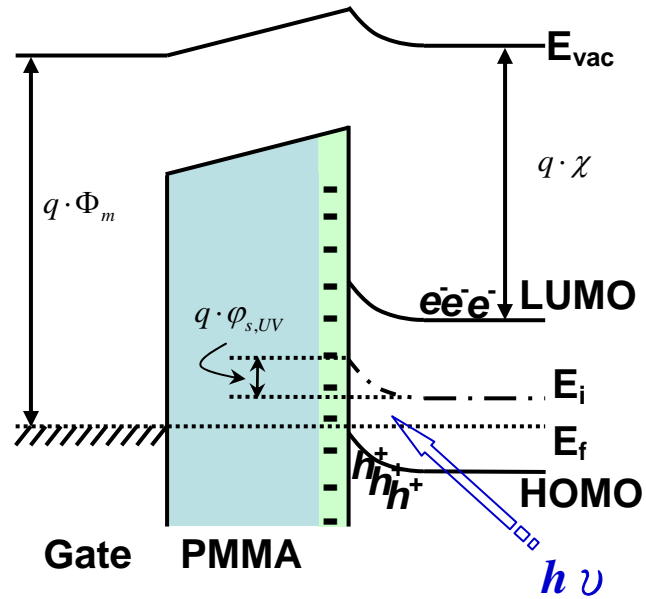


**Fig. 4-14(c)** When the illumination is continuously irradiated on OTFTs, due to the built-in electric field, electrons and holes will accumulate separately at the bulk and the interface of semiconductor layer and dielectric layer.

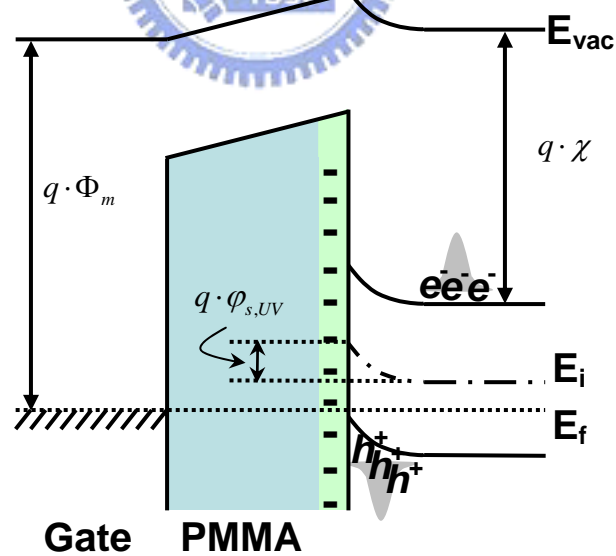


**Fig. 4-14(d)** Owing to the built-in electric field, the electrons and holes will be separated spatially. That will prolong the recovering time-constant.

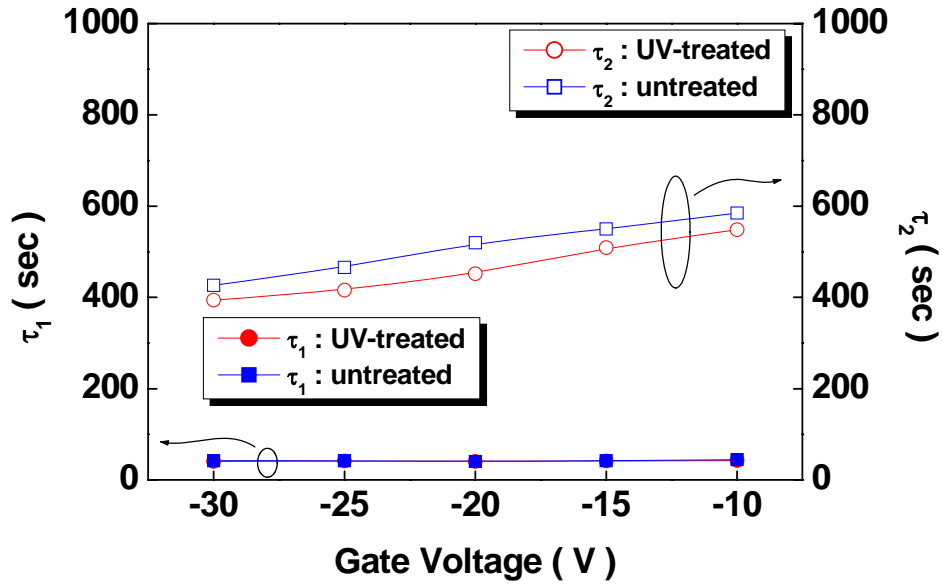


**Fig. 4-15(a)** Saturation time-constant of UV-treated PMMA-OTFTs and untreated PMMA-OTFTs is plotted as a function of gate voltage, respectively.

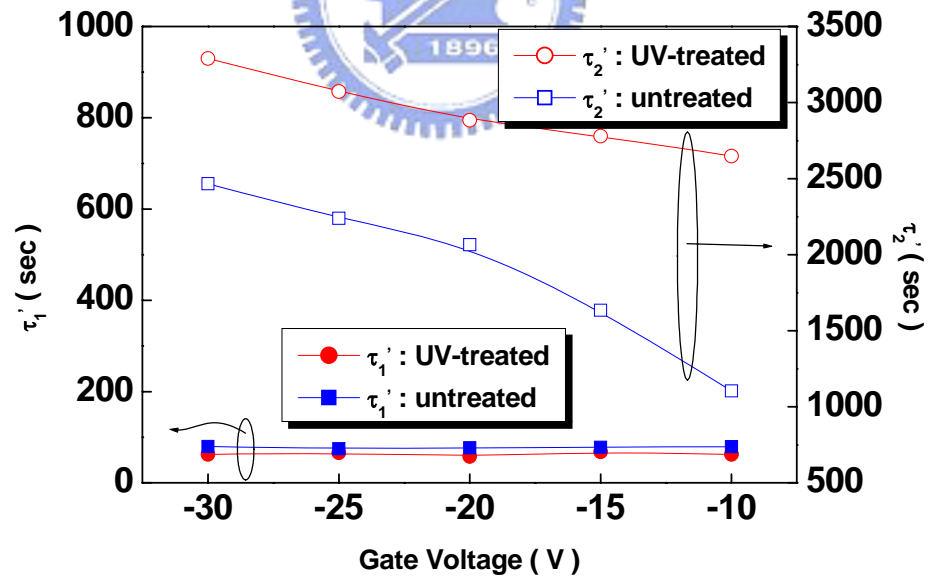


**Fig. 4-15(b)** Recovering time-constant of UV-treated PMMA-OTFTs and untreated PMMA-OTFTs is plotted as a function of gate voltage, respectively.

# 簡歷

姓名：顏睿志

出生年月日：中華民國七十一年三月三十日

住址：台北縣永和市民樂街 59 巷 14 號 3 樓

學歷：

私立淡江大學電機系 (2000.09~2004.06)

國立交通大學顯示科技研究所碩士 (2004.09~2007.06)

論文題目：

紫外光於 PMMA 有機薄膜電晶體之光響應提升研究

**UV-enhanced Photo responsivity on PMMA-OTFTs**